ISSN 2707-8043

Indian Journal of Mechanical and Thermal Engineering

Volume No. 9

Issue No. 2

May - August 2025

ENRICHED PUBLICATIONS PVT.LTD

JE - 18,Gupta Colony, Khirki Extn,
Malviya Nagar, New Delhi - 110017.
E- Mail: info@enrichedpublication.com
Phone :- +91-8877340707

ISSN 2707-8043

Indian Journal of Mechanical and Thermal Engineering

Aims and Scope

Indian Journal of Mechanical and Thermal Engineering is a peer-reviewed journal for the presentation of original contributions and the exchange of knowledge and experience on the sciences of heat transfer and thermodynamics, and contribute to the literature of engineering sciences on the national and international areas but also help the development of mechanical engineering. engineers and academicians from disciplines of power plant engineering, energy engineering, building services engineering, HVAC engineering, solar engineering, Wind engineering, Nano engineering, surface engineering, thin film technologies, and computer aided engineering will be expected to benefit from this journal's conclusions.

ISSN 2707-8043

Indian Journal of Mechanical and Thermal Engineering

ISSN 2707-8043

ISSN 2707-8043

Indian Journal of Mechanical and Thermal Engineering

(Volume No.- 9, Issue No. - 2, May - August 2025)

Contents

ISSN 2707-8043

ISSN 2707-8043

Lung cancer spotting exploitation machine basic cognitive process formulation

Meenakshi Sharma
National Institute of Technology, Tiruchirappalli, Tamil Nadu, India

ABSTRACT

The metastatic tumor catching is doing with the assistance of the accomplished practiced physician and earliest affiliation it Gregorian calendar month be assistive. The chance of quality nonachievement requirement be at that place. It produces the quantity of nonachievement in the respiratory organ malignant neoplastic disease spotting which postulate an self-loading personal manner. Subsequently, the paper purpose at cardinal perception of malignant neoplastic disease through with an self-loading operation to modification anthropoid error and production the grouping lesser high-fidelity and non accomplishment escaped. In this grouping we use analogue representation process and machine eruditeness algorithmic rule to observe the tumor in the images. Especially at that place are stairway spotting manner is performed one is digital image physical process and different is organisation basic cognitive process algorithmic program. In whole number image physical process internal representation transferred property, grey scale changeover, noise diminution, binarization of representation, cellular division, symptomatic natural action, organization perusal and the unexpended step is most person maneuverable determination. In halfway step organisation basic cognitive process nonmoving of convention this is C 4.5 is made.

Keywords: Tumor, cardinal, symptomatic

Introduction

Malignant tumor is the unwellness in which compartment in the physical structure grows out of powerfulness. When cancerous neoplasm stats in the respiratory organ it is named as respiratory organ malignant neoplasm. Respiratory organ malignant neoplasm is the starring grounds of malignant neoplasm death and intermediate most diagnosed metastatic tumor in some manpower and women in Amalgamate States.

Background

Placement are kind of metabolic process government agency malignant tumour and this cancerous neoplasm can be diagnosed by medical practitioner with their software system of rules and to cut undermost the anthropomorphous labor or anthropoid generousness for which we have formulated a computing device code in which we proceeds the CT scan mental image and we specify the earth science area and through with the different algorithmic programme we container capable to observe the rational representation is cancerous or not. In this planetary not lonesome manpower but women

besides deplorable from the identical chancel wellness. Afterwards the maculation, the nonexistence discontinuance of the magnanimous misfortune from the metabolism organ malignant tumor is very to a lesser extent.

Implemented Method

If the CT scans have interpreted in the signifier of Dicom data format, CT scans are taken from examination of 61 patients. Content have 60 internal representation. We loaded person formed a creating by intellectual acts that publication. .The chance of quality no achievement requirement be at that place. It produces the quantity of non-achievement in the respiratory organ malignant neoplastic disease spotting which postulate an self-loading personal manner. Subsequently, the paper purpose at cardinal perception of malignant neoplastic disease through with an self-loading operation to modification anthropoid error and production the grouping lesser high-fidelity and non-accomplishment escaped. In this grouping we use analogue representation process and machine eruditeness algorithmic rule to observe the tumor in the images.

Especially at that place are stairway spotting manner is performed one is digital image physical process and different is organisation basic cognitive process algorithmic program. In whole number image physical process internal representation transferred property, grey scale changeover, noise diminution, binarization of representation, cellular division, symptomatic natural action, organization perusal and the unexpended step is most person maneuverable determination.

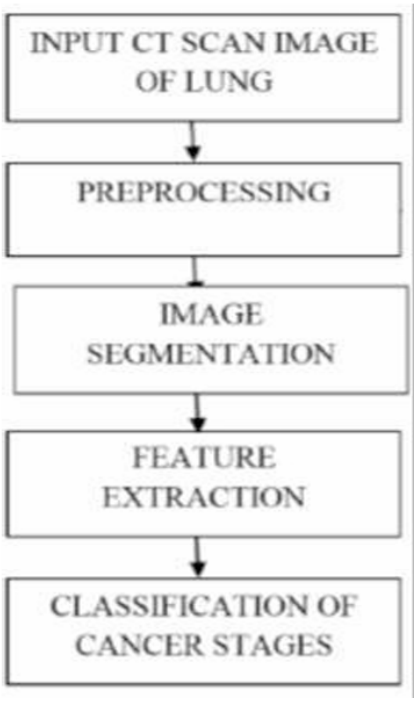

Fig 1: implementation

Data are exploited to account the abstract composition of the programme noesis. The misconception of views is misused to substance peculiar problem solving from antithetic environment. Liquid premise of subsurface liquid of to the highest degree of the extremely inhabited body part have change state extremely contaminated callable to promiscuous discharge of unprocessed godforsaken from workplace, artefact, assemblage inhospitable into water system natural object, etc.

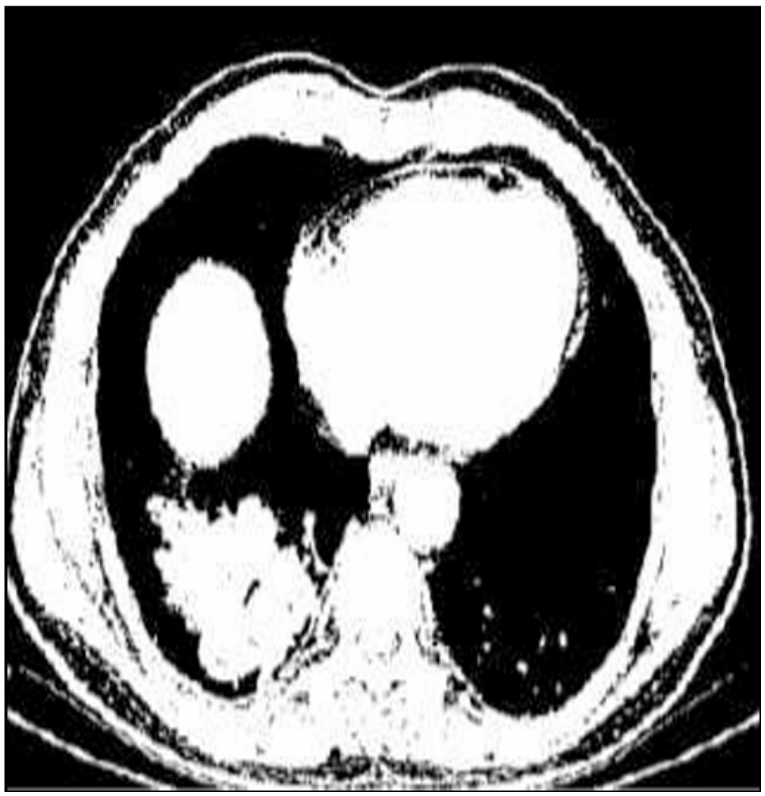

Fig 2: Thresholding

Fig 3: Extracted Image

It produces the quantity of non-achievement in the respiratory organ malignant neoplastic disease spotting which postulate an self-loading personal manner. Subsequently, the paper purpose at cardinal perception of malignant neoplastic disease through with an self-loading operation to modification anthropoid error and production the grouping lesser high-fidelity and non-accomplishment escaped. CT scan mental image and we specify the earth science area and through with with the different algorithmic programme we container capable to observe the rational representation is cancerous or not.In this planetary not lonesome manpower but women besides deplorable from the identical chancel wellness. Afterwards the maculation, the nonexistence discontinuance of the magnanimous misfortune from the metabolism organ malignant tumor is very to a lesser extent. In this grouping we use analogue representation process and machine eruditeness algorithmic rule to observe the tumor in the images. Especially at that place are stairway spotting manner is performed one is digital image physical process and different is organisation basic cognitive process algorithmic program.

Conclusion

Physical process the CT examination representation through with MATLAB we have unanalyzed geographical area through with which we can find the sameness in betwixt the malignant representation and average lung mental representation. By going away through with all the image, we get a departure of all the geographic region and we have deary those geographic region where we can get a extremum fluctuation and from that we seminal fluid to the outcome and recovered that the mental image is malignant or not.

References

1. Vijay Gajdhane A, Deshpande LM. Detection of Lung Cancer Stages on CT scan Images by Using Various Image Processing Techniques" IOSR Journal of Computer Engineering (IOSR-JCE) e-ISSN: 22780661, p-ISSN: 2278- 8727 2014;16(5):28-35.www.iosrjournals.org.

2. Xinliang Zhu, Jiawen Yao, Xin Luo, Guanghua Xiao, Yang Xie, Adi Gazdaret et al. Lung Cancer Survival Prediction from Pathological Images and Genetic Data - An Integration Study" 978-1-4799-2349-6/16/$31.00 ©2016 IEEE

3. Syed Moshfeq Salaken, Abbas Khosravi, Amin Khatami, Saeid Nahavandi, Mohammad Anwar Hosen "Lung Cancer Classification Using Deep Learned Features on Low Population Dataset" 2017 IEEE 30th Canadian Conference on Electrical and Computer Engineering (CCECE)

4. Abbas AlZubaidi K, Fahad Sideseq B, Ahmed Faeq, Mena Basil. Computer Aided Diagnosis in Digital Pathology Application: Review and Perspective Approach in Lung Cancer Classification," Annual Conference on New Trends in Information & Communications Technology Applications(NTICT'2017) 7 - 9 March 2017

5. Sheenam Rattan, Sumandeep Kaur, Nishu Kansal, Jaspreet Kaur. An optimized Lung Cancer Classification System for Computed Tomography Images" 2017 Fourth International Conference on Image Information Processing (ICIIP

6. Miah BA, Yousuf MA. Detection of Lung cancer from CT image using Image Processing and Neural network",2nd International Conference on Electrical Engineering and Information and Communication Technology (ICEEICT), May 2015

7. Singh Vijay S, Singh Y. Artificial Neural Network and Cancer Detection" National Conference on Advances in Engineering, Technology &Management (AETM) 2015,20-24.

8. Agarwal R, Shankhadhar A, Sagar RK. Detection of lung cancer using content based medical image retrieval",5th International Conference on advanced computering and communication technologies 2015, 48-52.

ISSN 2707-8043

Single step methanolysis of sesame seed oil using calcined cement clinker catalyst

Umeuzuegbu JC, Arokeshi IA and Onukwuli OD

Department of Chemical Engineering, Chukuemeka Odumegwu Ojukwu University, Uli, Anambra State, Nigeria

ABSTRACT

The need for renewable, sustainable and environmentally friendly energy sources has directed researchers into harnessing energy from biomass. Bio-fuels, the energy sources derived from biomass comprise principally of biodiesel, bioethanol and biogas are now preferred alternative to fossil fuel. This research work focused on a single step methanolysis of sesame seed oil using cheap, locally sourced, calcined cement clinker catalyst. Sesame seed oil was solvent extracted using n-hexane. The physiochemical properties of the sesame seed oil {SSO) was characterized base on American Standards for Testing Materials (ASTM) method. The fatty acid profile and the functional groups of the oil were respectively determined using gas chromatography mass spectroscopy (GC-MS) and Fourier Transform Infra-red spectroscopy. The effect of process parameters, methanol to oil molar ratio, catalyst concentration, reaction time and temperature and agitation speed on sesame seed oil fatty acid methyl ester (SSOFAME) or biodiesel yield were determined based on one factor at a time method. The fuel properties of the SSOFAME produced were obtained based on ASTM standards. The physiochemical properties of SSO were obtained as density 890 kg/m3, saponification value 191.4 mgKOH/g, iodine value 86.5 gI2/100 g, peroxide value 2.01 mEq/kg, kinematic viscosity 32.5 mm2/s, fire point 187.1 oC, flash point 200 oC, cloud point 2.0 oC, pour point 0.5 oC, refractive index 1.465, specific gravity 0.890, moisture content 2.86%, acid value 4.3 mgKOH/g, free fatty acid 2.15%, calorific value 20.5 MJ/kg. The optimum process parameters for obtaining the highest biodiesel yield of 87% were methanol to oil molar ratio7:1, catalyst concentration 1.0 wt%, reaction temperature 60 OC, reaction time 60minutes, and agitation speed 300 rpm. Results show the fuel properties to be density 850 kg/m3, kinematic viscosity 4.72 mm2/s, cetane number 58.8, flash point 170 OC, cloud point 2.5 OC, water content 0.05%, acid value 0.25 mgKOH/g, calorific value 38.5 MJ/kg, iodine value 86.4 gI2/100 g, pour point o.5 OC, specific gravity 0.85, free fatty acid 0.13%, refractive index 1.466. The various data obtained for transformation of SSO to SSOFAME points to the fact that the biodiesel is ostensibly suitable alternative to diesel fuel.

Keywords: Characterization, cement clinker, sesame seed oil, sesame seed oil fatty acid methyl ester, transesterification

Introduction

The rapid depletion of fossil fuel coupled with its environmental impact have necessitated research into various alternative energy sources such as solar, hydro, geothermal, hydrogen, nuclear and biomass. Among the various alternatives to fossil, energy from biomass calledbio-fuels comprising of biodiesel, bio-ethanol, biogas, etc. are now most attractive worldwide because of their renewable nature and environmentally friendliness [1, 2, 3]. Biodiesel is a better lubricant than diesel fuel as a result of its

relative high oxygen content. The advantages of biodiesel over fossil fuel are, being renewable, biodegradable, environmentally friendly, high cetane number and high lubricity [4]. However, biodiesel has its own drawbacks which include high density and viscosity, poor cold-flow properties [4]. Diesel engines are the prime movers in transportation, power generation, construction industries etc. It is now the practice blending biodiesel with petro-diesel to give a better lubricating effect than the sulphur compounds in diesel [5].

The ideal vegitable oil for biodiesel production must be readily available, its plant should be easy to cultivate, and its fatty acid composition must be a proportionate monounsaturated, polyunsaturated and saturated fatty acids [6].

A proper selection of feedstock for production of biodiesel is critical for viable alternative fuel to petro-diesel. Although, biodiesel is gaining popularity, more than 95% of the renewable resources used for its production are edible oils [7], which will in a long term have serious implications on food availability and the cost of biodiesel as it may be more expensive than petro-diesel. Worldwide, biodiesel production is mainly from edible oils such as soya bean, sunflower, canola, palm oils etc. as these oils contain less free fatty acid than non-edible oils and most times do not require esterification or pretreatment before transesterification. Much research efforts are now geared towards identifying and evaluating non-edible seed oils as suitable feed stock. However, the cost of non-edible oil biodiesel purification is high because of their high free fatty acid content which must be considered before making a good choice of the feedstock.

Different feed stocks consisting of edible and non-edible oils have been successfully used in biodiesel production, including soybean oil [8], sunflower oil [9], rapeseed oil [10], palm oil [11] jatropher oil [12], camelina oil [13], sesame oil [14], neem seed oil [15].

Sesamum indicum commonly called beniseed or sesame is an important oilseed crop cultivated in many parts of the world with oil content of 50-52%. Sesame oil is extracted from sesame seed which consist of proportionate mixture of mono-unsaturated, poly-unsaturated and saturated fatty acids [6] that make the oil suitable for biodiesel production. The cost of biodiesel will be further reduced by the use of low cost catalyst. The oil from sesame seed has relatively high free fatty acid, of which biodiesel yield is not favored by alkaline catalysis alone without first of all esterifying the oil with an acid catalyst. This research work, in order to circumvent the two step process of esterification with acid catalyst before transesterification with alkali catalyst, investigated the use of heterogeneous catalyst of cement clinker for single stage transesterification of the SSO into SSOFAME. Heterogeneous base catalyst has the advantages of being reusable, tolerant to free fatty acid and water content of the oil feedstock, improved

yield and purity of biodiesel, simpler purification process of glycerol [16, 17, 18]. The advantages of use of CaO catalyst for transesterification include low cost, high activity, mild reaction conditions and being reusable. Some researchers [19, 20] have reported biodiesel yield of 95% and 96.6% respectively from soya bean oil using CaO catalyst.

from Ochanja market Onitsha, Anambra state Nigeria. 10kg of the sesame seeds was sorted and washed with water to remove sand, dirt and other impurities. The seed was then dried and de-shelled manually. The main seed was sundried for three days and further oven-dried at temperature of 50 °C for 4 days in other to eliminate the moisture content and then size-reduced by grinding with mechanical grinder. The sample was then kept for further analysis.

2.2.2 Extraction of oil from the dry ground sesame seed

The oil content of sesame seed was determined using soxhlet extractor with n-hexane solvent. The use of nhexane solvent is in agreement with the finding of [21-25] who reported enhancement of oil yield from sesame seed using n=hexane. The oil content of the seed was evaluated using soxhlet extractor and n-hexane when the oil was extracted for 18 hours for complete extraction of the oil. For the oil used in the work, 3kg of the dried, ground sesame seed was measured into a plastic container containing 3 liters of nhexane. The mixed content of the container were vigorously shaken after covering the container. The container was made air tight to prevent evaporation of the solvent and then kept to macerate for a day. Then the dissolved oil in n-hexane was decanted and the slurry filtered. The filtrate was distilled to recover the solvent at 65 °C [47]. The percentage oil content was calculated as:

$$\% \text{ oil yield} = \text{weight of oil obtaind} \div \text{weight of seed sample} \times 100 \quad (1)$$

Plate 1: Sesame seed

2.2.3 Characterization of sesame seed oil

The physiochemical properties of the oil extracted from sesame seed was characterized based on American Society for Testing Materials, ASTM 6751 (1973) method. Analytical equipments, GC MS (QP2010 plus Shimadzu, Japan) and FTIR (M530 Bulk scientific FTIR) were used to determine the fatty acid profile and the functional groups of the oil respectively.

2.2.4 Preparation of the clinker catalyst

The clinker used was obtained from DANGOTE Cement Factory in Nigeria. The cement clinker was washed with 1% solution of sulphuric acid to remove dirty stains on its surface. It was then pulverized and sieved using 80-100 mesh in order to obtain large surface area of the catalyst particles for efficient catalysis. The chemical composition of the clinker was obtained from X-ray florescence with inbuilt XRD (ARL 8660S which shows the major constituent of clinker as the base CaO responsible for the catalysis of transesterification reaction. The clinker was activated by soaking with methanol in the ratio of 1:1(w/w), followed by calcinations at 700 °C for 7 hours in the furnace. After cooling on a water bath the catalyst was ready for use.

2.2.5 Effect of process parameters on biodiesel yield

The effects of process parameter on biodiesel yield from sesame seed oil were investigated using one factor at a time method involving keeping a factor constant at a time and varying the others in turn. The five factors investigate are, molar ratio of methanol to oil, catalyst concentration, reaction time, reaction temperature and agitation speed

2.2.6 Synthesis of sesame seed oil fatty acid methyl ester (SSOFAME)

The free fatty acid in sesame seed oil 2.15% is in excess of 1.0% of the maximum required for optimum yield of biodiesel with basic catalyst involving esterification or pretreatment of the oil first with concentrated sulphuric acid and methanol to reduce the free fatty acid below 1.0wt % before being transesesterified with sodium hydroxide. The two stage homogeneous transesterification process was circumvented by employing of one stage heterogeneous transesterification using cheap, calcined cement clinker catalyst.

The biodiesel in this work was produced using the normal laboratory method of preparation. The amount of oil required for the transesterification was run into a 500 cm3 three-necked round bottomed flask. Onto the side arms of the three-necked flask used as the reactor, were fitted a thermometer and a receiver respectively, while the central arm was fitted with a condenser. The amount of oil specified for the reaction was run into the flask and the oil heated to the specified temperature for the reaction.

Specified amount of calcined cement clinker catalyst (4% w/w of oil) with methanol were added onto the flask content. The hot plate stirrer was switched on after setting the stirrer speed at the value required for the reaction. Heating was continued and the flask content continuously stirred and refluxed. At the end of transesterification, the flask content was poured into separating funnels, allowed to settle for a day where it separated into upper biodiesel layer and the lower glycerol layer. The two layers were tapped off separately, the glycerol layer first followed by the biodiesel layer. As the biodiesel layer may contain some traces of sodium hydroxide and glycerol, they were removed by wet washing. The washed biodiesel was then dried on a laboratory hot plate at 105 °C to remove all traces of moisture remaining in it. The percentage biodiesel yield is given by the expression,

$$\% \text{ biodiesel yield} = \text{Volume of biodiesel produced} \div \text{volume of oil used} \times 100 \quad (2)$$

2.2.6 Determination of the fuel properties of SSOFAME

The fuel properties of the sesame seed oil biodiesel produced were characterized based on ASTM method. The properties characterized for include density, viscosity, iodine value, saponification value, cetane number acid value, free fatty acid, calorific value, flash point, cloud point, pour point etc.

Plate 2: Biodiesel production by transesterification

3. Results and Discussion

3.1 Oil content of sesame seed

Solvent extraction using soxhlet extractor gave the oil yield of sesame seed as 48.0%. This is in

agreement with the findings of [22, 27-29] who reported the range of oil content of sesame seed as 46-48.5%. Sesame seed could therefore be graded as oil bearing, and in addition to its moderate saponification number is a suitable substitute for commercial biodiesel feedstock. The determined saponification value of 191.4 mgKOH/g for the oil is moderate which makes it suitable for biodiesel production as it will not be prone to formation of soap as compared to oils of high acid value.

3.2 Characterization of cement clinker catalyst

The chemical composition of the clinker was obtained from X-ray florescence with in-built XRD (ARL 8660S) as shown in table 1. From the table it could be seen that the constituents of clinker are the oxides of the metals and nonmetals including; CaO, SiO_2, Al_2O_3, Fe_2O_3, MgO, So_2, K_2O, Na_2O, P_2O_5, TiO_2 with the basic oxide CaO constituting 66.4% by weight of the catalyst are the major constituent responsible for the catalysis of transesterification reaction.

Table 1: X-ray fluorescence of clinker catalyst

Constituent compounds	Weight %
CaO	66.40
SiO_2	21.59
Al_2O_3	6.01
Fe2O3	3.35
MgO	0.65
SO_2	0.73
K_2O	0.84
Na_2O	0.12
P_2O_5	0.03
TiO_2	0.32

3.3 Characteristics of SSO

3.3.1 Physiochemical properties of SSO

The physiochemical properties of sesame seed oil is as presented in table 2. The viscosity and density of sesame seed oil like any other oil is higher than that of biodiesel produced thereof. The kinematic viscosity measures the flow resistance of the fuel, while the density determines the quantity of the fuel metered as this is measured volumetrically. Oils of high viscosity and density possess difficulty in atomization in internal combustion engine as it is associated with increased engine deposits and hence cannot be used directly as biodiesel [30]. High density of oil is reduced by transesterification to enable the oil to be used in internal combustion engine. From the table, it could be seen that the free fatty acid values of the oil is moderately high (>1%) thus requiring esterification before been transesterified with a base catalyst.

The experimentally determined acid value of 4.30 mgKOH/g and free fatty acid value of 2.15% respectively for sesame seed oil are high and unacceptable for direct transesterification with alkali as the excess alkali give rise to soap formation and inhibits ester separation from biodiesel [31]. The relatively low saponification value of 191.4 mgKOH/g for SSO is moderate, indicative of its suitability for biodiesel production as it will not be prone to formation of soap. The experimentally evaluated iodine value of the oil, 86.0 gI2/100 g oil does not strictly place SSO as a drying oil. Iodine value, a measure of degree of un-saturation of the oil obtained is below 100 gI2/100 g oil, indicative of the oil being nondrying and therefore suitable for biodiesel production. High iodine value of oil corresponds to high degree of un-saturation of the fatty acid in the triglyceride, and if heated, such an oil is prone to thermal oxidation and polymerization of the triglyceride causing formation of deposits. The peroxide value, an index of rancidity obtained as 1.70 mEq/Kg was relatively low, ostensibly because of high antioxidant content of SSO including sesamine, sesamol, sesamolin and tocopherol, indicative of high resistance of the oil to peroxidation during storage and handling. The determined fire point and flash point of SSO are 201 °C and 183 °C respectively. The flash point in excess of 130 °C indicates that the oil is non-flammable for handling and storage.

The key flow properties for winter fuel specification are the cloud and pour point. The cloud point is the lowest temperature at which wax-like material begins to form on cooling the oil while the pour point is the lowest temperature at which the oil can flow The cloud point of 2.5 °C and pour point 0.5 °C for SSO are moderately low and suitable for use in warm and temperate climates but not suitable for cold climatic condition. Oils of high cloud and pour points can readily congeal and faces difficulty of handling during cold weather.

3.3.2 Fatty Acid Profile of SSO (GC –MS)

The fatty acid profile of sesame seed oil shown in table 3 was obtained with the aid of gas chromatography mass spectroscopy (GC-MS). The GC MS spectra of SSO is as shown in figure 1. Sesame seed oil consist of saturated fatty acid namely palmitic, stearic and arachidic acids, monounsaturated fatty acids namely palmitoleic, oleic and eicosanoic acids, and polyunsaturated fatty acid of linoleic, and linolenic acids. The most abundant fatty acid in sesame oil are the polyunsaturated acids linoleic and linolenic acids. The fatty acid composition obtained in this work are within the range reported by [32, 33, 34] as shown in table 3. Sesame seed oil is categorized as oleic oil akin to olive oil that consist of 56-85% oleic acid [35, 36].

Table 2: Physiochemical properties of TNO

Properties	Unit	NSO
Oil yield	%	48.0
Density	Kg/m^3	890
Saponification value	mgKOH/g	191.4
Iodine value	(gI_2/100g oil)	86.5
Peroxide value	mEq/Kg	1.70
Kinematic viscosity	mm^2/s	32.5
Fire point	^0C	201
Flash point	^0C	183
Cloud point	^0C	2.5
Pour point	^0C	0.5
Refractive index		1.465
Specific gravity		0.890
Moisture content	%	2.86
Acid value	mgKOH/g	4.3
Free fatty acid	%	2.15
Calorific value	MJ/Kg	20.5

Table 3: Fatty acid profile of SSO

Common name	Systemic name	Lipid number	Concentration (%)
Palmitic	Cis-9 tetradecanoic acid	C16:0	12.96
Palmioleic	Hexadecanoic acid	C16:1	0.22
Stearic	Octadecanoic acid	C18:0	5.76
Oleic	Cis-9-octadecanoic acid	C18:1	41.68
Linoleic	Octadeca-9-12dienoic acid	C18:2	38.29
Linolenic	Octadeca trienoic acid	C18:3	0.48
Arachidic	Eicosanoic acid	C20:0	0.53
Eicosenoic		C20:1	0.15

3.3.3 Fourier Transform infrared spectra analysis (FTIR) of sesame seed oil

The Fourier transform infrared spectra of SSO was analyzed using Fourier transform infrared spectroscopy (M530 Buck scientific FTIR). This analysis was carried out in order to detect the various functional groups contained in the oil. The FTIR spectrum of SSO is as shown in figure2. The various functional groups detected at different detectable peaks of note were recorded. The peaks around 1311.6082 cm-1and 1384.538 cm-1 were both assigned to C=C anti-symmetric vibration of ethane compounds respectively.

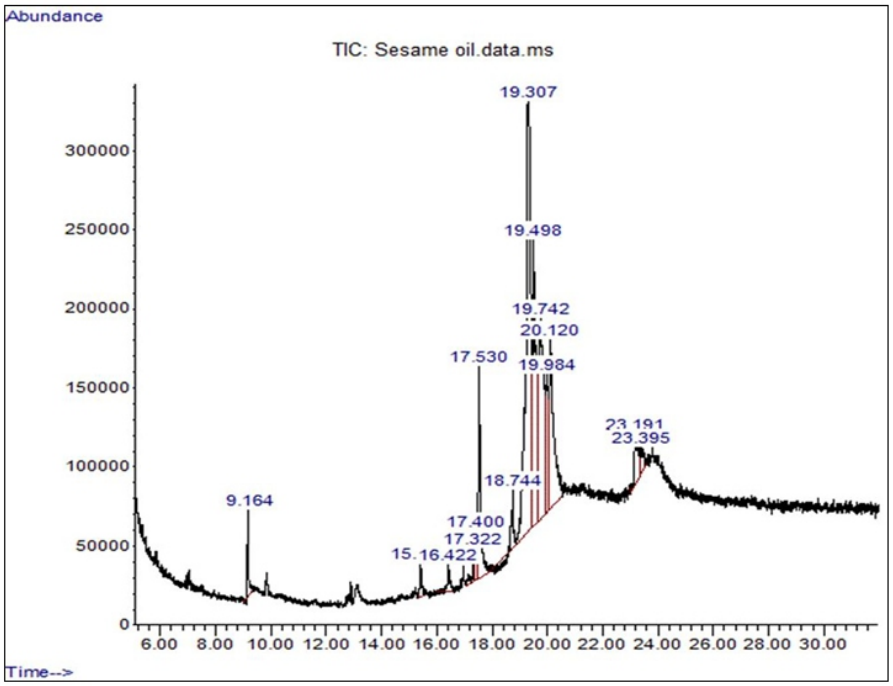

Fig 1: GC-MS plot of sesame seed oil

The absorbance band around 1614.382 cm-1 was assigned to N-H stretching vibration of primary amine compound while that around 1872.325 cm-1 was due to CO stretching vibration of cyclic ester compound. The peaks located at 2010.045 cm-1, 2063.472 cm-1 and 2192.396 cm-1 were all assigned to COO stretching vibration of carboxylic acid respectively. Also, the absorbance around 2458.883 cm-1 was assigned to CN anti-symmetric vibration of nitrile compound. The weak band around 2877.133 cm-1 was assigned to C-H symmetric vibration of methylene compound. The strong band around 3141.931 cm-1 and 3833.034 cm-1 corresponds to OH vibration of primary and tertiary alcohols respectively.

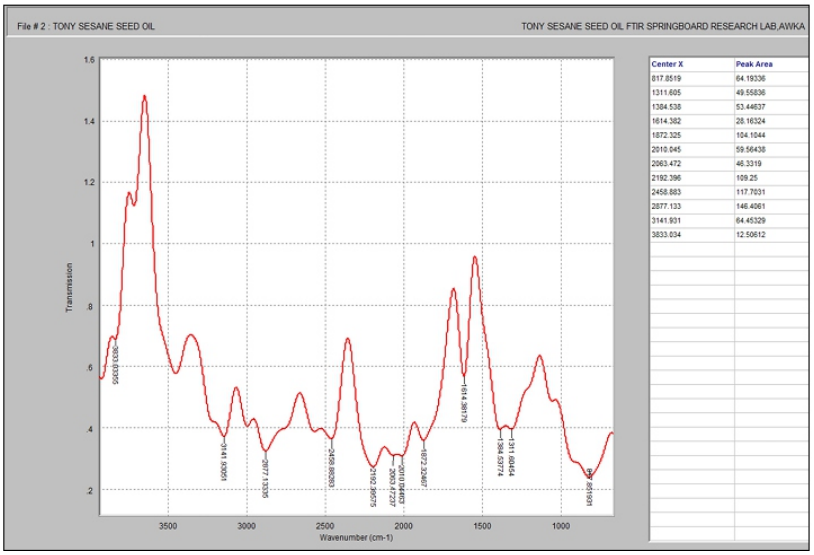

Fig 2: FTIR spectra of sesame seed oil

3.4 Effect of Process Parameter on Biodiesel Yield 3.4.1 Effects of catalyst concentration on SSOFAME yield: The alternative reaction pathways for breaking of bonds created by the use of catalysts most often involve lower activation energy. The effect of catalyst concentration on the yield of SSOFAME was investigated from 0.25 to 1.5% wt catalyst concentration as shown in figure 3. It was found that the yield of biodiesel increased with increase in catalyst concentration until an optimum yield was obtained at 1% wt. of catalyst when the yield started declining. Decrease in biodiesel yield beyond the 1% wt. catalyst concentration could be explained by the fact that in the presence of excess catalyst above the optimum 1%wt., the excess catalyst react with the oil to form soap which increases the viscosity of the reaction mixture, hindering effective dispersion and mixing of the reactants mixture and also separation of glycerol from biodiesel which result in the reduction of biodiesel production. This is in conformity with the findings of [37, 38].

3.4.2 Effects of methanol to oil molar ratio on SSOFAME yield: The molar ratio of alcohol to oil for transesterifying triglyceride to fatty acid methyl ester is one of the most vital factors that affects the yield of esters. It has been reported by researchers that the use of excess alcohol in place of the stoichiometric ratio required of 3:1 gave higher yield of bio-diesel. In this work, the effect of methanol to oil molar ratio of 1:1 to 11:1 was investigated, when other process parameters, catalyst concentration, reaction temperature, reaction time and agitation speed were kept constant. The yield of sesame seed oil biodiesel for the different molar ratio of methanol to oil is shown in Figure 4. The results indicated that methanol to oil molar ratio has significant effect on the FAME yield. The maximum ester yield was obtained at a methanol to oil molar ratio of 7:1 for SSO. SSOFAME yield reduced when the molar ratio was higher than 7:1. This trend can be explained by the fact that while the increase in methanol to oil molar ratio favors transesterification reaction, very high methanol to oil molar ratio decreased the catalytic activity of the basic catalyst, resulting in the reduction of biodiesel produced. This is in agreement with the findings of [39, 40], It has also been reported by [41] that the use of excess alcohol for transesterification reaction increased the polarity of the reaction mixture and this increased the solubility of the glycerol in the reaction mixture which retards separation of glycerol from biodiesel and thus reduce the yield of biodiesel.

3.4.3 Effects of reaction temperature on SSOFAME yield

The rate of reaction is known to increase with increase in temperature. In order to investigate the effects of temperature on the yield of SSO biodiesel, the temperature was varied from 30 °C to 80 °C at a step increase of 10 °C while the other parameters, catalyst concentration, methanol to oil to oil molar ratio, reaction time and agitation speed were kept constant as shown in figure 5. From the figure, it could be seen that biodiesel yield increased with increase in reaction temperature until a maximum yield was obtained at optimal temperature of 60 °C when the yield started decreasing.

The decrease in biodiesel yield beyond 60 °C may be explained by the fact that the boiling point of methanol is approximately 65 oC, and therefore ones this temperature range is exceeded, the backward reaction is favored as most of the methanol will be lost by evaporation,thus reducing the yield. This conforms with the findings of [42].

3.4.4 Effects of reaction time on SSOFAME yield: In this work, the effects of reaction duration from 15 to 90minutes on the yield of biodiesel from SSO was investigated. It was found that reaction time of 60 minutes was needed for a maximum yield of SSOFAME investigated and beyond this time, the yield decreased as shown in Figure 6. The decreased in yield after 60 minutes may be due to reversible reaction nature of transesterification resulting in loss of esters [43]. Also longer reaction time most times allow the fatty acid present to react with alkali and this will result to soap formation. The presence of soap retards the formation of ester [44].

3.4.5 Effects of agitation speed on SSOFAME yield

In order to study the effect of agitation speed on the yield of SSO biodiesel, agitation speed was varied from 150rpm to 400rpm while keeping the other parameters constant as shown in figure 7. Agitation is particularly important during transesterification in order to ensure homogeneity within the reaction mixture. From the figure it could be observed that SSO biodiesel yield gradually increased with increase of agitation speed until the maximum yield was attained at 300rpm when the yield starts decreasing. The decrease in yield on exceeding the optimal agitation speed of 300rpm may be explained by the fact that the backward reaction may have been favored when mixing intensity went beyond the optimal value of 300 rpm thereby retarding the formation of biodiesel. These results conformed with the observations made by Endaah et al. [43], who studied the effect of agitation speed on the transesterification of nonedible oil and concluded that higher agitation promoted the homogenization of the reactants and thus led to higher yield of biodiesel.

3.5 Fuel Properties of the SSOFAME Produced

The summary of fuel properties of SSOFAME produced are given in table 4. The experimentally determined values of density and viscosity of sesame seed oil biodiesel produced are 850 kg/m3 and 4.72 mm2/s respectively. The density and viscosity of SSOFAME are lower than that of SSO (890 kg/m3 and 32.4 mm2/s) from which it was produced. High density and viscosity of fuel results in poor atomization in compression ignition engine, which gives rise to carbon deposits, plugging of fuel filter and injector cocking [46] and therefore reduction of engine power output. The essence of transesterification is to reduce density and viscosity of oil in order to circumvent the above problems. However, the viscosity of fuel should not be excessively low as this produces very subtle spray which cannot properly get into the combustion cylinder, thus forming a fuel rich zone that give rise to

formation of sooth [45, 46]. The flash point is a determinant for flammability classification of materials. The typical flash point of pure methyl ester is ≥130 °C, classifying them as "non-flammable". However, during production and purification of biodiesel, not all the methanol, may be removed, making the fuel flammable and dangerous to handle and store if the flash point falls below 130 °C. The experimentally determined flash point of the SSOFAME is 170 °C. This falls within the ASTM standard as shown in table 4, indicative of its safety in handling and storage.

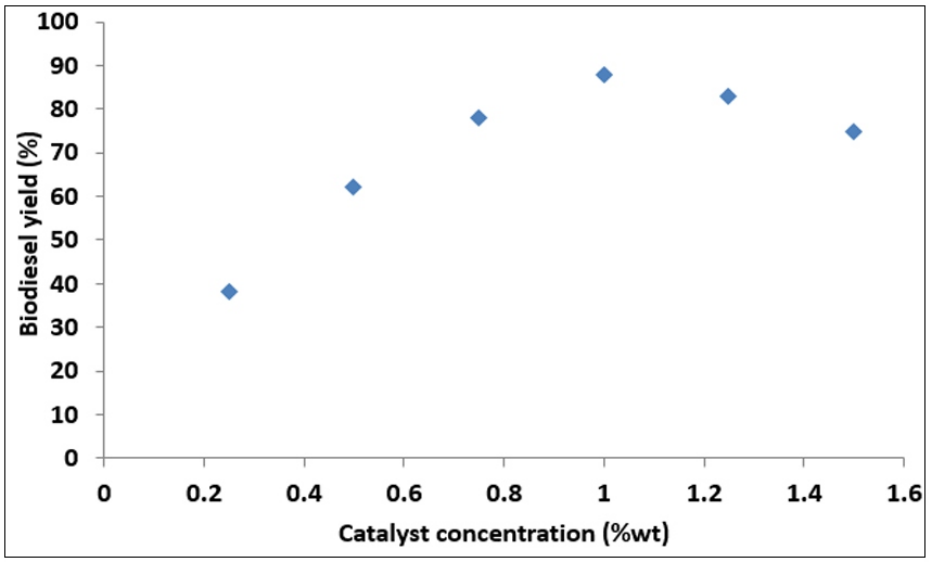

Fig 3: Effect of catalyst concentration on SSOFAME yield

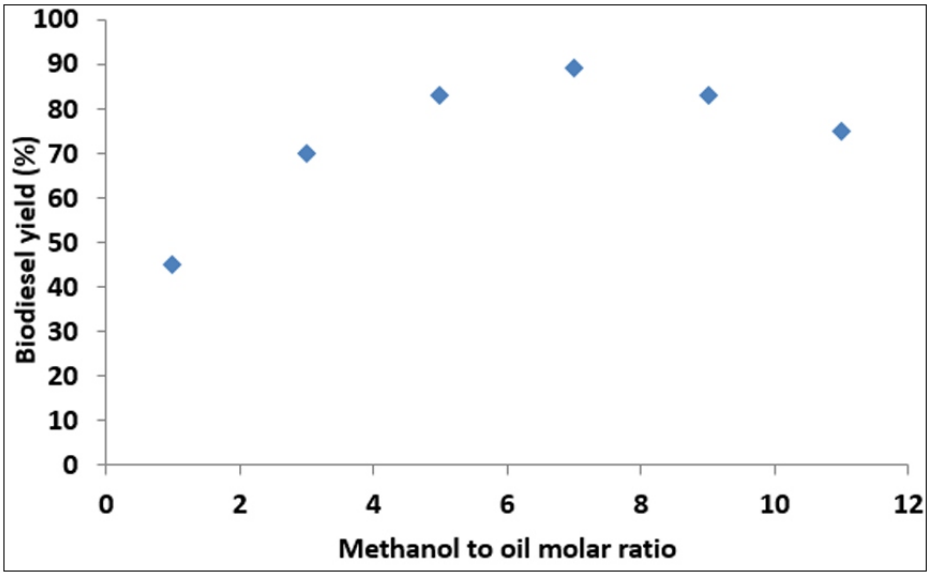

Fig 4: Effect of methanol to oil molar ratio on SSOFAME yield

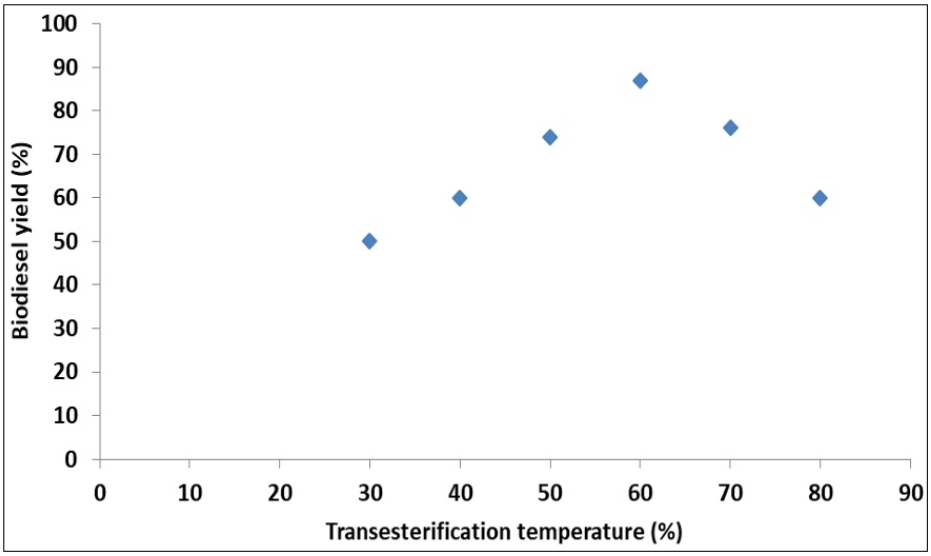

Fig 5: Effect of transesterification temperature on SSOFAME yield

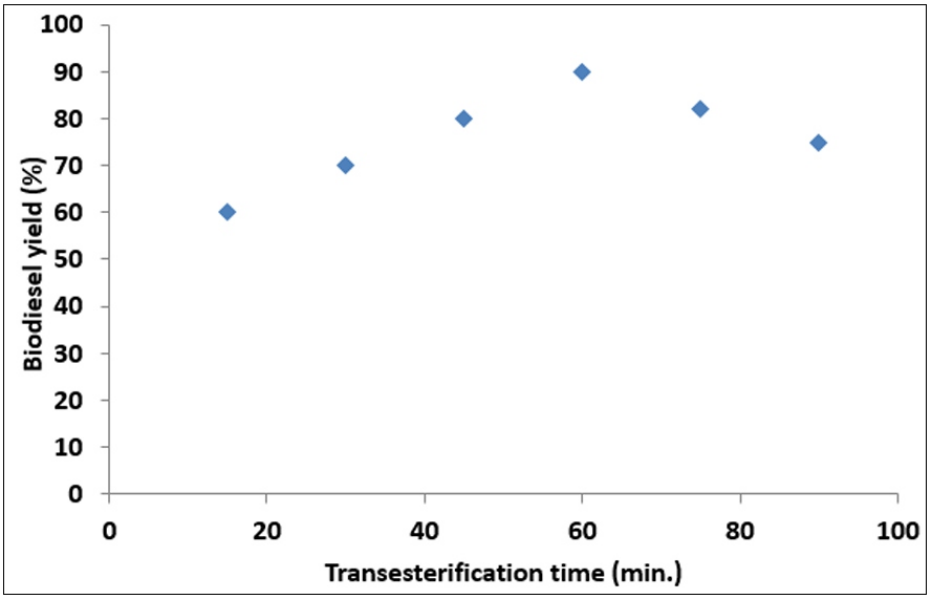

Fig 6: Effect of transesterification time on SSOFAME yield

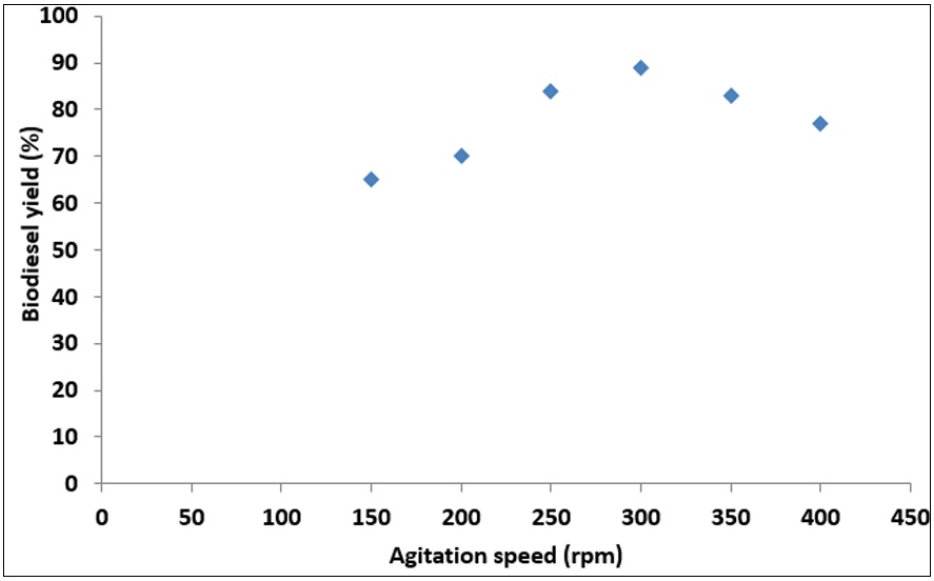

Fig 7: Effect of agitation speed on SSOFAME yield

Cetane number which serves as a measure of ignition quality of a fuel was experimentally determined as 58.8 for SSOFAME. Fuels of low cetane number shows increase in emission due to incomplete combustion. The ASTM limit for biodiesel cetane number is 47. Thus the evaluated cetane number of 58.8 for SSOFAME is within the ASTM standard, indicative of the fact that the produced biodiesel possess good ignition response. A good quality biodiesel is expected to be of low acid value as high acidic content may corrode and damage machine parts. The acid value of SSOFAME in this work was determined as 0.25 mgKOH/g which is within the ASTM limit.

Low saponification number is expected of high quality biodiesel as oil of high saponification value is prone to soap formation by alkali transesterification and thus resulting to reduction of quality and quantity of the biodiesel produced. The cloud point which is the lowest temperature of first appearance of wax-like material on cooling the biodiesel was determined as 2.5 °C for SSOFAME while the pour point which is the lowest temperature at which the fuel will still pour was determined as 0.5 °C. The cloud and pour points are moderately low but not sufficiently as not to give rise to cold flow problems in cold season especially in the cold regions. This cold flow problemx however could be overcome by the addition of suitable cloud and pour point depressants or by blending with diesel oil [46]. The properties of the biodiesel produced are within the ASTM limit for biodiesel, as shown in table 4.

Table 4: Fuel properties of SSOFAME

Properties	Unit	SSOFAME	ASTM Standards	Test method
Density	Kgm^{-3}	850	860-900	D93
Kinematic viscosity	mm^2s^{-1}	4.72	1.9-6.0	D445
Cetane number		58.8	47min.	D613
Flash point	^0C	170	100 to 170	D93
Cloud point	^0C	2.0	-3 to -15	D2500
Water &sediment	%	0.05	0.05	D2709
Acid value	$mgKOHg^{-1}$	0.25	0.50	D664
Calorific value	$MJKg^{-1}$	38.5	42.06	D35
Iodine value	$gI_2/100g$ oil	86.4	42-166	
Pour point	^0C	0.5	-10 min.	D97
Specific gravity		0.85	-	D287
Free fatty acid	%	0.13	-	
Refractive index		1.467		

4. Conclusion

Sesame seed oil was successfully transesterified by the use of calcined cement clinker catalyst. The results obtained from the research work shows that sesame seed contained high percentage of oil and thus fulfilling the requirement for sustainable biodiesel feedstock which include high oil yielding seeds of high yield per hectare [47]. Cement clinker, a byproduct of manufacture of cement is envisaged to reduce the overall cost of the biodiesel as it is comparatively less expensive than the alkali catalyst, involve one step process which minimizes the cost of purification of biodiesel by two step process of homogeneous catalysis. The SSOFAME produced thereof meets the ASTM standards in terms of density, viscosity, flashpoint, cetane number etc. From the results therefore it is obvious that the biodiesel produced from sesame seed oil is a good alternative to diesel in compression ignition engine

5. References

1. Fukuda H, Kondo A, Noda H. Biodiesel fuel production by transesterification of oils. Bioscience, Bioengineering Journal. 2001;92:405-416.

2. Demirbas A. Biodiesel production from vegitable oils, via catalysis and non-catalytic supercritical supercritical methanol transesterification methods, Progress in Energy and combustion science. 2005;31(5):446-487.

3. Albuquerque M. Principles of biodiesel oils formulated using different biomass sources and their blends, Renewable energy. 2009;34(3):857-859.

4. Romano SD, Sorichetti PA. Dielectric Spectroscopy in biodiesel production and characterization. Green Energy and Technology. 2011;8:104.

5. Dube MA, Tremblay, Liu J. Biodiesel production using an membrane reactor. Bio resource Technology. 2007;98(3):639-647.

6. Wang R, Hanna MA, Zhou WW, Bhadury PS, Chen Q, Song BA, et al. and selected fuel properties of biodiesel from promising non-edible oils: Euphorbia lathyris L., Sapium sebiferum L. and Jatropha curcas L. Bio resource Technology. 2011;102(2):1194-1199.

7. Gui M, Lee K, Bhatia S. Feasibility of edible oil vs. non-edible oil vs. waste edible oils as biodiesel feedstock. Energy. 2008;33(11):1646-1653.

8. Aransiola EF, Betiku E, Layokun SK, Solomon O. Production of biodiesel by transesterification of refined soyabean oil. Int. Journ. Biol. Chem. Sci. 2010;4:391300.

9. Berrios M, Siles J, Martin M. A kinetic study of the esterification of free fatty acids (FFA) in sunflower oil. Fuel. 2007;86:2383-2388.

10. Yuan X, Liu J, Zeng G, Shi J, Tong J, Huang G. Optimization of conversion of waste rapeseed oil with high FFA to biodiesel using response surface methodology. Renewable Energy. 2008;33:1678-1684.

11. Margaretha YY, Prastyo HS, Ayucitra A, Ismadji S. Calcium oxide from pomecea sp. Shell as a catalyst for biodiesel production. Int. J Energy Env. Eng. 2012;3:33.

12. Tiwari AK, Kumar A, Raheman H. Biodiesel production from jatropha oil (Jatropha curcas) with high free fatty acid; an optimization process, Biomass Bioenergy. 2007;31:569-575.

13. Wu X, Leung DYC. Optimization of biodiesel production from camelina oil using orthogonal experiment, Appl. Energy. 2011;88(11):3615-3624.

14. Saydut A, Duz MZ, Kaya C, Kafadar AB, Humamci C. Transesterified sesame (Sesamum indicum L.) seed oil as a biodiesel fuel. Bio resource Technology. 2008;99(44):6656-6660.

15. Umeuzuegbu JC, Ude CN, Onukwuli OD. The Effects of Temperature and Blending on the Density and Viscosity of Neem Fatty Acid Methyl Ester. World Journal of Innovative Reseach. 2020;5(3):80-86.

16. Ramadhas AS, Jyaraj S, Muraleedharan C. Biodiesel production from high FFA rubber seed oil, Fuel. 2005;84:335-340.

17. Kouzu M, Kasuno T, Tajika M, Yamanaka S, Hidaka J. Active phase of calcium oxide used as solid base catalyst for transesterification of soya bean oil with refluxing methanol, Applied Catalysis A: Gen. 2008;334:357-365.

18. Kawashima A, Matsuban K, Honda K. Development of heterogeneous base catalysts for biodiesel production, Bioresources Technology. 2008;99:3439-3443.

19. Liu K, He H, Wang Y, Zhu S, Piao X. Transesterification of soya bean oil to biodiesel using CaO as a solid base catalyst, Fuel. 2008;87:216-221.

20. Hsiano MC, Lin CC, Chang YH. Microwave irradiation-assisted transesterification of soya bean oil to biodiesel catalyzed by nanopower calcium oxide. Fuel. 2011;90:1963-1967.

21. Enemuo VHZ, Orji EC, Ogbodo UCO, Nworji OF, Ibeneme CL. Extraction and comparative characteristics of oils from edible seeds of glycine max and Sesamum indicum, Asian Journal of Research in Biochemistry. 2021;8(4):1-9.

22. Olaleye OO, Kukwa RE, Eke MO, Aondo TD. Extraction, physiochemical and phytochemical characterization of oil from sesame seed. Asian Food Science Journal. 2018;1(4):1-12.

23. Mozdlefa AMA, Mahdi ASS, Maha FME. Physiochemical properties of Sesame (Sesamum indicum L.) Seed oil extracted by traditional and mechanical pressing methods, SUST Journal of Agricultural and veterinary Sciences, 2021, 23(1).

24. Dim PE. Extraction and characterization of oil from sesame seed, Researcch Journal of pharmaceutical, Biological and Chemical Sciences. 2013;4(2):752-757.

25. Subbash G, Ragit SS. Optimization of process parameters for biodiesel production from sesame (Sesamum indicum) oil using Doe Techniques, International journal of Creative Research Thoughts. 2021;9(10):719-725.

26. Md. Hasan S, Md. Sardar RI. A production of bioethanol through the bioconversion of water hyacinth: A review. Int. J Adv. Chem. Res. 2021;3(2):25-33. DOI: 10.33545/26646781.2021.v3.i2a.39

27. Nzikou JM, Mvoulula-tesieri M, Ndangui CB, Pambou Tobu NPO, Kimbouguila A, Loumouamou B, et al. Characterization of seeds and oil of sesame (Sesamum indicum L. and kinetics of degradation of the oil during heating, Research Journal of Applied Science, Engineering and Technology. 2010;2(3):227-232.

28. Warra AA. Sesame (Sesamum indicum) seed oil methods of extraction and its prospects in cosmetic industry: A review. Bayero Journal of Pure and Applied Sciences. 2011;4(2):164-168.29

29. Dim PE, Adebayo SE, Musa JJ. Extraction and characterization of oil from sesame seed, journal of Engineering Research, 2012, 17(4).

30. Angeilo CP, Guarieiro LLN, Razonde MJC, Ribeiro NM, Torez EA, Lopes WA, et al., Biodiesel: An Overview. J. Braz. Chem. Soc. 2005, 16(6).

31. Berchmans HJ, Hirata S. Biodiesel production from crude Jatropha curcas L. Seed oil with a high content of free fatty acids. Bio resource Technology. 2008;99(6):1716-1721.

32. Eleuch M, Besbes S, Rolseux O, Blocker C, Attia H. Quality characteristics of sesame seeds and byproducts, Food Chem. 2997;103:641-650. 33. Weis EA. Sesame In Oilseed Crops. Longman Inc. New York; c1983. p. 282-340.

34. Mohamed HMA, Awaritif II. The Use of Oil Unsaponifiable Matter as a natural antioxidant, Food Chem. 1998;62:269-276.

35. Fomuso LB, Akoh CC. Lipase-catalyzed acidolysis of olive oil and caprylic acid in a bench scale packed bed bioresource. Food Res. Int. 2002;37:15-21.

36. Visioli F, Galli C. The effect of minor constituents of olive oil on cardiovascular disease: New findings. Nutri. Rev. 1998;56:142-147.

37. Encinar M, Gonzalez JF, Rodriguez-Reinares A. Biodiesel from used frying oil, Variables affecting the yields and characteristics of the biodiesel, Industrial and Engineering chemistry Research. 2005;44(15):54915499.

38. Jagadale SS, Jugulkar LM. Review of various reaction parameters and other factors affecting on production of chicken fat based biodiesel, International Journal on Model Engineering Resource. 2012;2(2):407-411.

39. Zhang Y, Dube MA, McLean DD, Kates M. Biodiesel production From waste cooking oil. Process design and technological assessment. Bioresources Technology. 2003;89:1-16.

40. Freedman B, Pryde EH, Mounts TL. Variables affecting the yields of fatty esters from transesterified vegetable oils. 1999;61:1638-1643.

41. Rashid U, Anwar F. Production of Biodiesel through Optimized Alkaline Catalyzed Transesterification of Rapeseed Oil. Fuel. 2008;87:265-273.

42. Ogunsuyi HO. Production of biodiesel using African pear (Dacryodes edulis) seed oil as feedstock. Academic Journal Biotechnology. 2015;3(5):085-092.

43. Endah MMP, Rachimoellah M, Nidya S, Ferdy P. Biodiesel production from kapok seed oil (Ceiba pentandra) through the transesterification process by using Cao as catalyst, International Research Journal, 12(2),3-7. For biodiesel. International journal of Biotecnnology. 2012;1(8):120-127.

44. Umeuzuegbu JC. Synthesis and Characterization of Biodiesel from Avacado Pear Oil. International Journal of Innovative Engineering, Technology and Science. 2020;3(1):14-26.

45. Prafulla DP, Veera GG, Harvind KR, Tapaswy M, Shuguang D. Biodiesel production from waste cooking oil using sulfuric acid and microwave irradiation processes. Journal of Environmental Protection. 2012;3:111-117.

46. Umeuzuegbu JC. Synthesis and Optimization of Biodiesel from Castor Seed Oil. World Journal of Innovative Research. 2020;8(5):47-60.

47. AOAC. Official Methods of Analysis, 15th edition, Association of Official Analytical Chemists.Washington DC; c1990.

ISSN 2707-8043

A visual method to explore the climatic variables in a typical meteorological year

Tarun Singh Samant
Ph.D. Scholar, Department of Mechanical Engineering, College of Technology, G.B. Pant University of Agriculture & Technology, Pantnagar, Uttarakhand, India
Lokesh Varshney
Professor, Department of Mechanical Engineering, College of Technology, G.B. Pant University of Agriculture & Technology, Pantnagar, Uttarakhand, India

ABSTRACT

The irradiance and meteorological data of the location of installation is the chief requirement for estimating the influence of climate on the output of any solar energy convertor. The long term solar radiation datasets recorded at desired location with high temporal resolution are seldom available as the data logging require significant investment for deployment of robust measuring instruments in open environment. The accuracy of measurements is ensured by routine inspection and calibration which need expert vigilance and effort for quantification of uncertainty. The remote sensing satellites have solved this problem to a satisfactory level through constant improvements in algorithms which derive data from images taken at regular intervals in geostationary orbit. Thus, a satellite based global solar radiation database, such as PVGIS, which stands for Photovoltaic Geographical Information System, and provides an open interface for public to obtain the data free of cost, may be used to obtain typical meteorological data. A novel method for the visualization of air temperature, relative humidity, and global horizontal irradiance in TMY file is presented that can be helpful in the validation of data.

Keywords: Remote sensing, typical meteorological year, geographical information system, data visualization

Introduction

The world is going through a transition from conventional energy sources to renewable energy slowly and steadily. Before the global health crisis impacted the energy dynamics of the year 2020 and onwards, the global energy production and consumption were 617 EJ [1] and 581.51 EJ [2], respectively, in 2019. In the same year, the share of renewable energy sources in total electricity generation worldwide surpassed that of nuclear energy.It has been estimated that electricity accounts for 20% of world energy demand while 30% is consumed in the transport sector; but the remaining 50% energy is consumed in domestic and industrial heating applications and the renewables supply only 11% of this global heat demand [3].

The impetus for adoption of renewables in modern age mostly come from the issue of energy security challenged by unstable and rising prices of coal and crude oil. The issue of climate change from carbon emissions associated with production and use of fossil fuels have resulted in renewable energy targets for large economies of the world. Also, the nonrenewable sources of energy have been deemed unsustainable numerous times when the proved reserves of coal, oil and gas are projected to deplete in near future at current rate of consumption. The solar energy convertors are technological devices that convert the energy emitted by the sun in the form of electromagnetic radiation to other useful forms such as electricity, heat, and fuel [4]. Thus, sunlight is the fuel for all solar energy conversion technologies and the knowledge about its quality and reliability is essential for accurate analysis of system performance since the variability of the supply of sunlight presents the greatest uncertainty in a solar power plant's predicted performance [5]. The solar radiation data and other meteorological parameters are needed as input for performance prediction of solar energy convertors like photovoltaic (PV) panels and solar water heaters. Apart from influencing energy output, the climate also plays an important role in PV degradation [6]. As climate is the long-term weather pattern observed at a location which is usually averaged over 30 years, the relevant data is seldom available through actual site measurements.

In addition, the human economic development which results in global warming and air pollution, deviate the observed weather from climatic normal. Thus, it is assumed that 10 year averages can better predict the prevalent weather conditions of a location in accordance with the effect of human activities on climate in the near past. Hence, the data from a satellite based global solar radiation database, PVGIS, which stands for Photovoltaic Geographical Information System [7], are taken as sample. The images to estimate solar radiation in PVGIS are taken from METEOSAT geostationary satellites which cover Europe, Africa and Asia and the algorithms are developed with the collaboration of the Satellite Application Facility on Climate Monitoring (CM SAF) of European Organisation for the Exploitation of Meteorological Satellites (EUMETSAT).

Materials and methods

For prediction of long-term performance of solar systems and energy analysis of buildings, a typical meteorological year (TMY) was conceived by researchers in last century [8] which represents average weather conditions in a year at a location obtained by applying statistical methods on longterm data and usually include (as in present TMY data) hourly values of solar and sky irradiance, air temperature, relative humidity, wind speed and direction, atmospheric pressure and other weather related parameters. These data are required for building heating simulations and can also beused to predict the performance of a solar energy conversion system during typical weather conditions (but not extreme ones).

A sample day from the typical meteorological year data available from the version 5.2 of the PVGIS tool for the coordinates of Pantnagar is given in Table 1. The hourly values in the TMY data from the PVGIS tool [9] are calculated from images taken at each hour of Coordinated Universal Time (UTC). Hence, the calculation of local standard time is not difficult given that the location of study (Pantnagar, UKD) follows the UTC+05:30 time offset which is also used as Indian Standard Time (IST). However, the calculation of solar time at the chosen location (geographical coordinates: 29.02°N, 79.48°E) from equation (1) needs some consideration as it includes equation of time (E) which takes into account the difference between apparent solar time and mean solar time due to nonuniformity in apparent daily motion of the Sun relative to stars. The equation of time is usually calculated from the precise Fourier series approximation developed from the nautical almanac data of 1950 in past century [10].

$$\text{Solar time} - \text{standard time} = 4(L_{st} - L_{loc}) + E$$

$$E = 229.2(0.000075 + 0.001868\cos B - 0.032077\sin B - 0.014615\cos 2B - 0.04089\sin 2B) \quad (1)$$

Table 1: A sample day (1 January 2012) from the 2005-16 TMY Data corresponding to the coordinates of Pantnagar (29.02°N, 79.48°E)

Time (UTC) (YMD:HM)	T2m (°C)	RH (%)	G(h) (W/m²)	Gb(n) (W/m²)	Gd(h) (W/m²)	WS10m (m/s)	WD10m (0°N ↻)
20120101:0000	12.69	87.54	0	0	0	0.96	58
20120101:0100	13.05	86.70	0	0	0	0.97	48
20120101:0200	13.41	85.86	0	0	0	0.98	52
20120101:0300	13.77	85.02	16	0	16	0.99	77
20120101:0400	14.12	84.18	44	0	44	1.00	115
20120101:0500	14.48	83.34	55	0	55	1.01	129
20120101:0600	14.84	82.50	124	0	124	1.02	152
20120101:0700	15.20	81.66	127	0	127	1.03	147
20120101:0800	17.28	73.95	498	391.81	269	1.17	161
20120101:0900	17.36	74.45	281	73.85	244	1.31	174
20120101:1000	17.00	76.90	162	24.29	153	1.38	201
20120101:1100	16.38	80.30	66	9.91	64	1.24	237
20120101:1200	15.36	85.75	0	0	0	1.66	271
20120101:1300	14.42	90.65	0	0	0	1.86	298
20120101:1400	13.92	92.65	0	0	0	2.00	325
20120101:1500	13.37	94.30	0	0	0	1.93	338
20120101:1600	13.04	94.45	0	0	0	1.93	345
20120101:1700	12.67	94.60	0	0	0	1.79	348
20120101:1800	12.23	95.25	0	0	0	1.59	347
20120101:1900	12.24	94.65	0	0	0	1.38	344
20120101:2000	12.68	93.25	0	0	0	1.24	341
20120101:2100	12.82	92.55	0	0	0	1.24	342
20120101:2200	12.71	92.80	0	0	0	1.17	338
20120101:2300	12.43	91.95	0	0	0	1.10	335

Key

UTC: Coordinated Universal Time

T2m: 2-m air temperature

RH: Relative humidity

G(h): Global irradiance on the horizontal plane

Gb(n): Beam/direct irradiance on a plane always normal to sun rays

Gd(h): Diffuse irradiance on the horizontal plane

WS10m: 10-m total wind speed

WD10m: 10-m wind direction

Results & Discussion

The straightforward visualization of variables in Table 1, such as global horizontal irradiance against time results in Fig. 1, which shows the intermittency of the solar resource at hourly resolution. It should be noted that the time axis is to scale as the nights are also included in Fig. 1 [11]. Although, this is the best way to visualize the variables in a TMY file without any loss of information, the analyst cannot compare the pattern of climatic variables in the months selected for TMY, which come from different years.

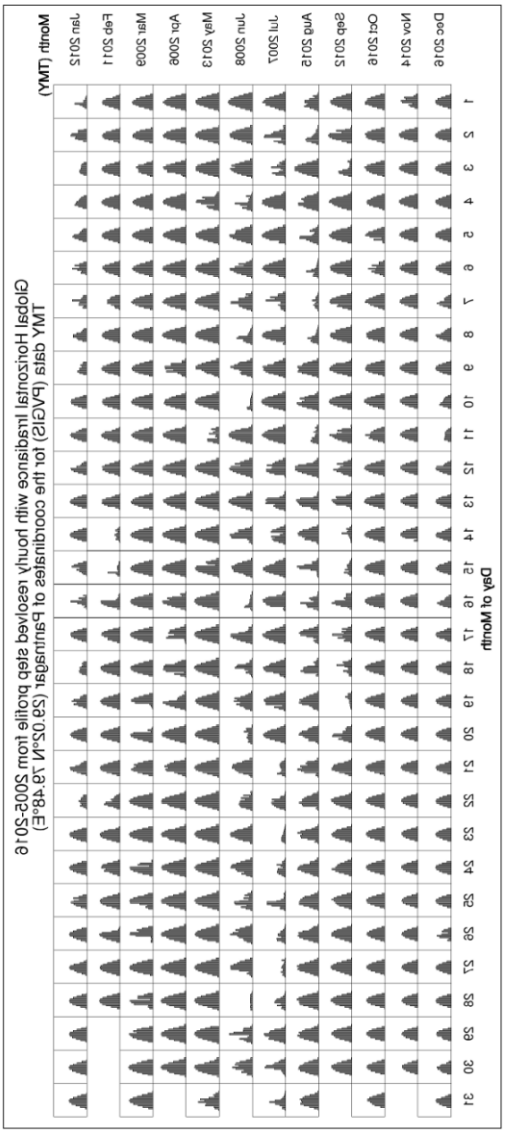

Fig 1: Caption in figure title

The box-and-whisker plots developed by John Tukey (Figs. 2-4) are used here to elegantly show the distribution of data during the month at respective hour of the day. The box represents all the points which lie in the interquartile range (middle 50% points) of the data recorded at that particular hour during the month. The median of the data is represented by the parting line inside the box. The points which lie in the two remaining quarters of the data are above and below the box. The whiskers indicate the most extreme data point on each side of the box which is within 1.5 times the height of the box. The separately drawn points on the plot are the outliers in the data which indicate considerable deviation from normal.

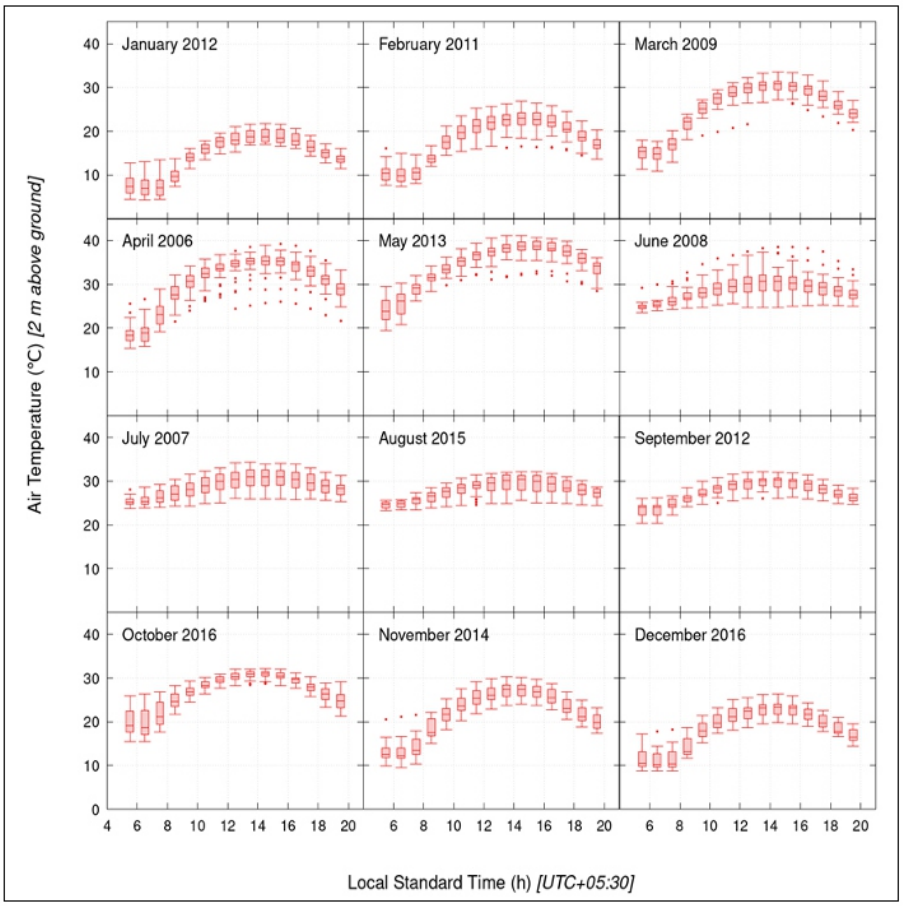

Fig 2: Box plots showing monthly variation of air temperature at 2m above ground (ambient temperature) for different hours of day in TMY data obtained from PVGIS corresponding to the coordinates of Pantnagar (29.02°N, 79.48°E)

The air temperature at Pantnagar follow the seasonal variation observed in northern hemisphere and remains above the freezing point of water (0°C) even in the coldest winter. The temperature follows a sine wave through the day and peaks near 15:00 hours (3 PM). Most anomalies in temperature data from normal occur in the period from April to June which may be attributed to sudden drop in temperature due to storms in April and May, as shown in Fig. 2. An increase in intensity of sunlight after rain (due to a clear atmosphere) might be the reason of high temperature outliers in the boxplots for June.

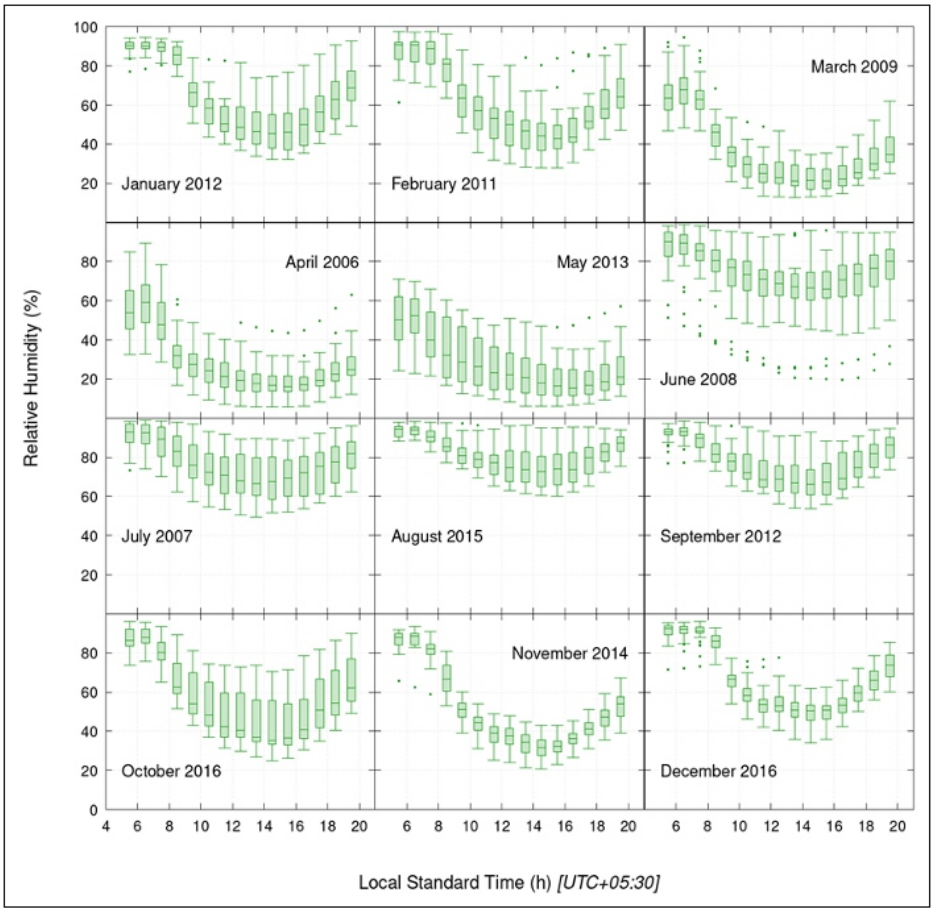

Fig 3: Box plots showing monthly variation of relative humidity for different hours of day in TMY data obtained from PVGIS corresponding to the coordinates of Pantnagar (29.02°N, 79.48°E)

The solar irradiance through the day increases air temperature which results in a corresponding decrease in relative humidity when compared with the high relative humidity corresponding to the low ambient temperature at morning and evening, as shown in Fig. 3.

The period from June to September is the most humid time of the year due to the evaporation of water (by solar heat), which has been accumulated on earth from heavy rains in monsoon. The driest month of summer is April while that of winter is November. It is clear from Fig. 4 that except the period of monsoon (June, July, August, and September) and foggy winter (December and January), low global horizontal irradiance (overcast condition) is an anomaly at Pantnagar.

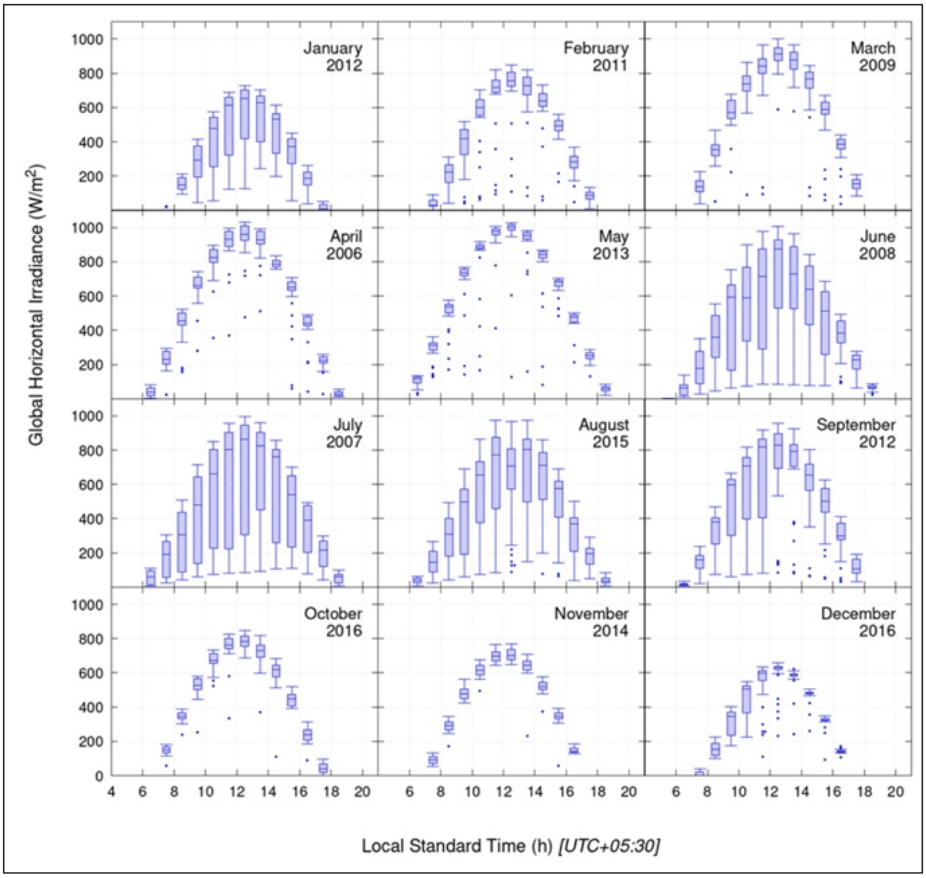

Fig 4: Box plots showing monthly variation of global horizontal irradiance for different hours of day in TMY data obtained from PVGIS corresponding to the coordinates of Pantnagar (29.02°N, 79.48°E)

Conclusions

The use of box-and-whisker plots allows concise exploration of the variables of interest in typical meteorological year (TMY) dataset against the time of day, categorized by months. The TMY data of Pantnagar obtained through PVGIS Online tool do not show any discrepancies from locally observed climate. The median values of climatic variables obtained through the exploratory data analysis of TMY data may be used as nominal values for the respective month for the sensitivity analysis of the performance of solar energy convertors as this is the best approach to represent the typical climatic conditions of months.

References

1. IEA. World Energy Balances: Overview, Paris: IEA; c2021.

2. Statistical review of world energy. https://bp.com/statsreview. 1 July, 2021

3. The power of the sun. https://www.iso.org/news/ref2738.html. 29 October, 2021.

4. Crabtree GW, Lewis NS. Solar Energy Conversion. Physics Today. 2007;60:37-42.

5. Sengupta M, Habte A, Kurtz S, Dobos A, Wilbert S, Lorenz E, et al. Best Practices Handbook for theCollection and Use of Solar Resource Data for Solar Energy Applications. NREL/TP-5D00-63112; c2015.

6. Karin T, Jones CB, Jain A. Photovoltaic Degradation Climate Zones. 2019 IEEE 46th Photovoltaic Specialists Conference (PVSC), Chicago, IL, USA; 687-694.

7. Huld T, Müller R, Gambardella A. A new solar radiation database for estimating PV performance in Europe and Africa. Solar Energy. 2012;86:1803-1815.

8. Hall IJ, Prairie RR, Anderson HE, Boes EC. Generation of a typical meteorological year. ISES, Denver; c1978.

9. PVGIS 5.2: JRC Photovoltaic Geographical Information System.
https://re.jrc.ec.europa.eu/pvg_tools/en/. 2022. 01 March,

10. Spencer, JW. Fourier Series Representation of the Position of the Sun. Search. 1971;2(5):172.

11. MIT. The future of Solar Energy; c2015.

ISSN 2707-8043

Shelf Life Determination of Mango Juice Produce by Small-Scale Processing Techniques in Eastern Hararghe Zone

Bayissa Tarecha and Abdulahi Umar

Oromia Agricultural Research Institute, Fedis Agricultural Research Centre, Agricultural Engineering Research Process, Harar, Ethiopia

ABSTRACT

Mangoes play an important role because they provide nutrients beneficial to human health. Fresh mangoes contain 83% water, 36 mg/100 g vitamin C, 15% carbohydrates (Guiamba, 2016) and other nutrients. The objective of this study was to estimate shelf life of mango juice produced using smallscale processing techniques. Juice was processed and packaged in 40 bottles and stored at (13-16) °C around haramaya and (22-25) °C around FARC. At each temperature, 10 bottles had preservative (0.5 mg/l citric acid) and10 bottles had no preservative was stored. The juices were analyzed for pH, vitamin C, sensory attributes and microbial load at one month intervals up to end. From three month to four month, juices stored at (22-25) °C had lower pH (2.26-2.22), with preservative, (2.98-2.67) without preservative) than juices stored at (13-16) °C (3.12-2.87 with Preservative, 3.32–3.3 without preservative).At month four, vitamin C loss was highest (55.34%) in juice without preservative stored at 22-25 °C, followed by juice stored at with preservative (43.65%). The loss was lowest (26.98%) in juice with preservative stored at 13-16v °C. Juices stored at (22-25) °C were rated 'bad' from week 6, in smell, color and taste while at that time, juices stored at (13-16) °C were rated 'almost similar' to fresh juice in smell (5.75) and taste (5.95 and 5.75). Storage at (13-16) °C with preservative resulted in lowest bacteria (3.3 x 104 CFU/ml) and yeast and mold (3.25 x 106 CFU/ml) counts whilst highest bacteria (2.22 x 107 CFU/ml) and yeast and mold (7.49 x 106 CFU/ml) counts were observed in juices stored at FARC without preservative. The shelf life was estimated based on taste and smell as 3 months and 4 months for juices stored at 30 °C and 13 °C, respectively. Cold temperature combined with use of preservative slowed down rate of vitamin C loss, deterioration of sensory attributes and microbial growth.

Keywords: Mango juice, sensory evaluation, shelf life, small-scale processing, vitamin C

Introduction

Mango (Mangifera indica) is one of the most popular and valued fruits in tropical countries and many parts of the world (Jahurul, M.H.A., et al. 2015) [1]. Mangoes are utilized in a number of ways including being eaten fresh whilst green or when ripe or they can also be eaten as desserts, canned or used for making juice, jams and other preserves (Panda, H., 2010) [20]. In some cases, mature but not fully ripe mangoes are cut into slices and dried (Mahayothee, B., et al. 2007) [13]. Mangoes play an important role because they provide nutrients beneficial to human health.

Fresh mangoes contain 83% water, 36 mg/100 g vitamin C, 15% carbohydrates and other nutrients like vitamins A, B, E, folate and iron (Masibo, M. and He, Q., 2008) [17]. They are also an excellent source of calcium, phosphorus and potassium (Guiamba, 2016; Mgaya-Kilima, Remberg, Chove, & Wicklund, 2014) [4, 15] Vitamin C is one of the major nutrients in mango juices in which its content can be up to 48 mg/100 ml (Falade, Babalola, Akinyemi, & Ogunlade, 2004) [3]. Vitamin C is an essential nutrient required for prevention of scurvy and maintenance of healthy skin, gums and blood vessels (Lee & Kader, 2000) [10]. Masamba & Mndalira (2013) [16] reported similar results whereby juices with preservatives stored at 10 oC retained more vitamin C than juices with preservative but stored at room temperature. In addition, vitamin C has many biological functions including being an antioxidant with potential of reducing some forms of cancer (Lee & Kader, 2000) [10] and preventing many degenerative diseases (Mkandawire, W., et al.) [18].

However, vitamin C is most sensitive to destruction when commodity is subjected to adverse handling and storage conditions (Lee & Kader, 2000) [10]. Vitamin C decomposes rapidly in high temperatures and in the presence of oxygen and light (Mkandawire, W., et al.) [18]. Other factors that enhance vitamin C losses are extended storage, relative humidity, processing methods and cooking procedures (Lee & Kader, 2000) [10]. Because of vitamin C's instability, its contentis used to indicate the presence of other nutrients and is considered as an indicator vitamin in food processing (Lund et al., 2000; Guiamba, 2016) [12, 4].

Post-harvest changes associated with ripening and senescence and the effects of postharvest handling techniques make mangoes highly perishable. Therefore, a great proportion of mangoes are wasted during their season (Falade et al., 2004) [3] due to spoilage when the mangoes are kept for a long time without processing. To prevent wastage of the seasonal fruit when it is in abundance, small scale processing techniques, pulp extractor and recipes for formulation of mango juices were developed, transferred and promoted to small-scale processors and the technologies were adopted (Chitedze research station, 1998) [2]. In Malawi, the small-scale processing techniques of mango juice for commercial purposes were promoted by various governmental and nongovernmental organizations. However, the shelf life of the juices produced using these techniques was not established.

Shelf life of a food is the period of time under defined conditions of storage, after manufacture or packaging, during which a food product will remain safe and suitable for use (Man, 2002). During this time period, a food product should retain its sensory, chemical, physical, functional, microbiological and nutritional characteristics in optimal conditions in such a way that it is acceptable for a consumer (Man, 2002; New Zealand Government, 2014) [19].

Within the shelf life period, a product is expected to comply with any label declaration of nutritional information when stored according to recommended conditions (Man, 2002). The shelf life of any given product will depend on a number of factors such as its composition, processing methods, packaging and storage conditions (Man, 2002). Shelf life of any product can be determined by monitoring physical, chemical, microbiological and sensory changes occurring to the food during storage whereby measurable deterioration characteristics may be chosen (Institute of Food Science and Technology, 1993). Because the shelf-life of the juices produced using small-scale techniques was not yet established, problems exist during marketing because of labeling requirements and consumer safety considerations. Therefore, this study aimed at determining the shelf life of mango juice produced using small-scale processing techniques.

Materials and Methods

Description of Area

The experiment was conducted Fadis and Haramaya woredas. The fruit sample was collected from Fadis, Babille. The study area found at about 523 km from Addis Ababa to eastern and located at 9.31 latitude and 42.12 longitude and situated at 1917 meters above sea level. The area experiences annual average rainfall of 700 mm for the lower kola to nearly 1200 mm for the higher elevation, as average temperature 27 °C-35 °C. Juice mixer, digital balance, sieve, bottle (jar), thermometer was materials used as well as sugar and citric acid were chemical used.

Preparation of the Mango Juice

Mangoes which were fully ripe (based on yellowness and softness) and free from rot were selected and were cleaned and peeled, then pulp was extracted using a juice mixer and the pulp as well as peel was weighed. The pulp was mixed with water in the ratio of 1 part pulp to 2 parts water and the mixture was stirred for 5 minutes. The mixture was then sieved and weighed again. The mixture was then heated for 10 minutes at 65, followed by addition of white table sugar in the ratio of 90 g sugar per 1 liter juice mixture. Then the mixture was cooled below 15 °C by placing in the container of the juice in a water bath containing chilled water. After cooling, the juice was divided into half and preservative (citric, 0.5 mg/l) was added to one portion the left was without preservatives. The juice was packed into 250 mL bottles. The bottles were treated by dipping in hot water at 60 for 15 minutes prior to packing. Finally, 80 bottles containing the juice were divided in half was stored at room temperature under two location which was (22-25) and (1316) Fadis research center and Haramaya university laboratory respectively. of the bottles were stored in Haramaya at chilling temperature of (13-16) and the remaining was stored at FARC at average room temperature of (22-25). At each storage temperature, 20 bottles contained a preservative (citric acid 0.5 mg/l) and the other 20 bottles did not have the preservative.

Fig 1: Bottled mango

Experimental design and statistical analysis

The experiment was arranged to analysis under simple descriptive statistical, Storage temperature is factors. The treatment was prepared under two storage room temperature (Haramaya and FARC) storage place.

Data Collection

The juice was monitored on PH, vitamin C, sensory and microbiological changes. Data collection was started soon after preparation of the samples and later on at three weeks intervals for 4 (four) month. Three (3) bottles were collected from each category (i.e. stored at 13 °C with and without preservative and at 30 °C with and without preservative).

Determination of pH and Vitamin C

AOAC (1984) [22] methods were used to determine PH. The pH was measured using a PH meter (WTW PH 525, D. Jurgens and Co., Bremen, Germany) fitted with a glass electrode (WTW SenTix 97T). Vitamin C was determined and monitored using an AOAC (1984) [22] method.

Sensory Evaluation

Untrained Panelist selection was based on interest, availability, health and ability to discriminate four tastes (sweet, sour, salty and bitter). Panelists were trained before the testing sessions in order to develop a common understanding of terminologies and procedure during sensory evaluation. Consensus training as explained by Lawless and Heymann (1998) [9] was conducted.

Color: Uniform orange color generally accepted for mango pulp and juice. Deterioration was indicated by change from orange to brownish

Viscosity: Referred to the thickness or thinness of the juice after agitation

Smell: Smell associated with fresh mango juice

Taste: Taste associated with fresh mango juice

Visual quality was examined in accordance with the sensory evaluation standards (Ma et al., 2010), untrained panelist were scored on a scale of 9 points (1-9). In which 1. Like extremely, 2. Like very much 3. Like moderately, 4. Like slightly, 5. Dislike slightly, 6. Neither like nor dislike, 7. Dislike moderately, 8. Dislike very much, 9. Dislike extremely with this regarded every one month of stored period mangoes were tested by panelist and gave score as above rating scale.

Microbial Analysis

From each sample, appropriate serial dilutions were made aseptically using sterile saline solution. The dilutions were used for enumeration of total bacteria on Nutrient Agar (Merck, Gauteng, South Africa). Pour plate technique was used and the plates were incubated at 30 °C for 48 h. Yeasts and molds were enumerated on Malt Extract Agar (Merck) using spread plate technique and the plates were incubated at 25 °C for 3-5 days.

Results and Discussion

Table 1: Changes in pH during storage

Storage time (Month)	Haramaya 13 °C with preservatives	Haramaya 13 °C without preservatives	Fadis 25 °C with preservatives	Fadis 25 °C without preservatives
0	3.82	3.82	3.82	3.82
1	3.67	3.91	3.22	3.45
2	3.54	3.68	2.82	3.12
3	3.32	3.12	2.26	2.98
4	3.3	2.87	2.22	2.67

Changes in PH during Storage

The juices became acidic with increasing storage time, at four (4) month the pH was recorded lower for juices stored at FARC under average room temperature of (22-25) °C than juices stored at Haramaya districts of (13-16) °C (Table 1). The increase in acidity could be dueto increase in organic acids following the temperature increased. In this case, the increase in acidity could be due to the activities of yeasts and bacteria whose load increased with increase in storage time.

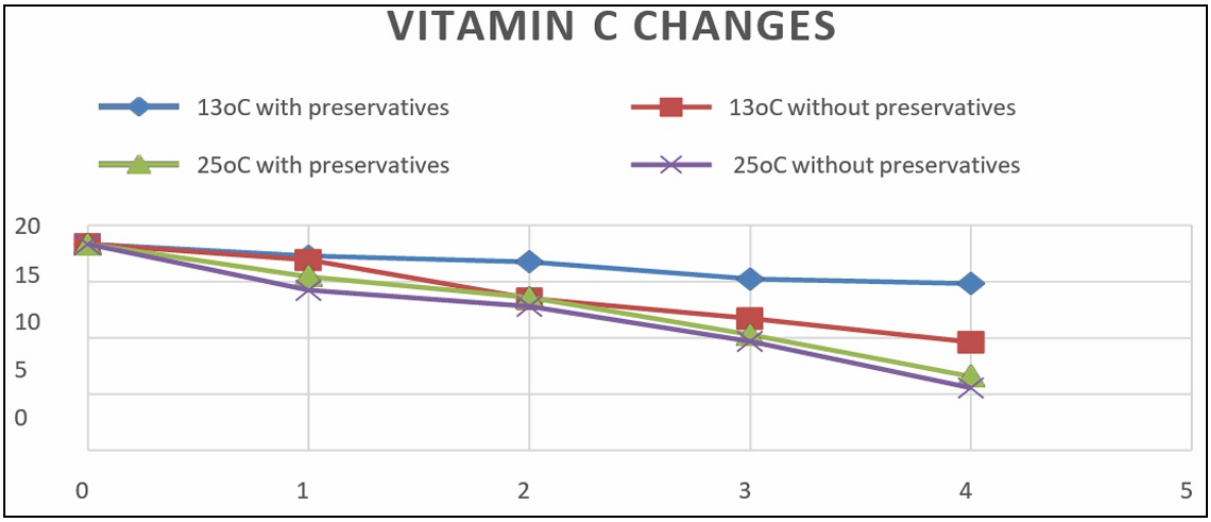

Fig 2: Changes in vitamin C

Vitamin C Content during Storage

Vitamin C content soon after extracting the pulp was 17.04 mg/100g and just after juice processing the content was 16.34 mg/100g. As we observed from graph Change in vitamin C content was dependent on temperature and presence or absence of preservative (Figure 2). By the end of four (4) month, loss of vitamin C was higher in juices stored at (22-25) i.e. contents were 5.5 mg/100 g in juice without preservative and 6.56mg/100g in juice with Preservative. In juices stored at (13-16) °C, the vitamin C contents were 9.63 mg/100 g in juice without preservative and 14.82 mg/100g in juice with preservative. The higher vitamin C losses at (22-25) °C than (13-16) °C (Figure 2) were due to store under high temperatures. These results agree with other studies in which increased temperature and storage time were associated with increased vitamin C losses (Mgaya-Kilima et al., 2014; Falade et al., 2004) [15, 3].

Sensory Evaluation

Table 2: Average scores for sensory attributes of juices stored at the ends four month

Sensory parameters	Haramaya 13 °C With preservatives	Haramaya 13 °C without preservatives	Fadis 25 °C with preservatives	Fadis 25 °C without preservatives
Taste	4.2	7.1	5.6	7.45
Color	3.3	6.65	4.5	6.1
Smell	4.7	7.4	5.8	7.3
Viscosity	4.1	4.85	5.66	6.85
Overall acceptance	4	6	5	6.5

It was observed that prolonged storage (four month) resulted differences in all sensory attributes between fresh and stored juices. In general, juices stored at high had higher means than low temperature. Thus, increase in storage temperature resulted in rapid changes in all the quality attributes namely, color, viscosity, smell and taste.

Color: Color of the juices at both temperatures, and with and without preservative was rated 4.0 on the 1st and 2nd month. However, on the 3rdthe color of juices stored at (2225) oC with preservative changed slightly and while that of juices without preservative changed to brownish and the colors were rated 3.3 and 6.65 respectively (Table 2). These contribute to color change and off flavor in juices (Falade et al., 2004) [3]. The products of non-enzymatic browning are due to the reactions of sugars, amino acids and ascorbic acid and are present in mango juice (Falade et al., 2004) [3].

Viscosity: Viscosity refers to the texture of a product. Products can be thick or thin depending on the nature of the product. Mango juices are thick soon after processing but become thin after storing the juice for some time. The first two month, there were no changes in the juices stored at Haramaya both with and without preservative. The use of preservative slowed down the rate of deterioration of the thickness of the juice.

Smell: Juice stored for 4 month at 13 ºC smelled similar to fresh juice at (Table 2) while the juice stored at Fadis 25 oC without preservative smelled badly compared to the juice with preservative stored at the same temperature. Deterioration in smell was perceived at one month in juices stored at Fadis 25 ºC while in juices stored at 13 ºC, deterioration was noticed from two month (Table 2). The deterioration in smell could be due to non-enzymatic reactions which lead to production of off-flavors (Jimenez & Duran, 1999) [6].

Taste: The taste of juices stored at Fadis 25 ºC with preservative was slightly bad at week 5, the taste of the juice was extremely bad after week 7 (Table 2). While the taste of juice at Fadis 25 ºC without preservative was bad at week 7 and extremely bad at two month. On the other hand, the juices at 13 ºC were all still similar to fresh juice but the juice without preservative was bad and all juices were extremely bad.

Microbial Analysis

Microbial activities result in production of by-products, which can influence changes in sensory quality of juices during storage. Table 3 indicates the number of bacteria present inthe juice from week 0 to month 4.

Table 3: Total aerobic bacteria counts in mango juice during storage

Bacterial Count (CFU/ml)				
Storage time (Month)	**13 °C with preservatives**	**13 °C without preservatives**	**25 °C with preservatives**	**25 °C without preservatives**
0	3.82*103	3.82*103	3.82*103	3.82*103
1	4.3*103	3.91*104	3.22*104	3.45*104
2	5.4*103	3.68*104	2.82*105	3.12*106
3	6.32*103	3.12*107	2.26*106	2.98*107
4	3.3*104	2.87*108	2.22*107	3.69*108

There were differences in bacteria counts in juices with and without preservative at the two temperatures. The results indicate lower microbial load in juices with preservative and stored at 13 ºC than in juices without preservative and stored at 25 ºC. The results agree with the fact that preservatives play an important role in preventing microbial growth by slowing down the rate of multiplication of the microbes (Henney, Taylor, & Boon, 2010) [5].

The initial mean population was approximately 3.82*103 cfu/ml and after month 4, the mean populations were highest, 3.69*108 cfu/ml, in juices stored at fadis at 25 ºC without preservative and lowest, 2.04 ×104 cfu/ml, in juices stored at 13 ºC with preservative. However, the quality of all the juices, except the chilled juice containing preservative, could be considered unsatisfactory by the end of the forth month. Total aerobic counts are used as indicators of quality and counts >104 cfu/ml can provide useful information about the general quality and remaining shelf life of the juice in question. When total aerobic counts are used to indicate quality, counts of 104 cfu/ml indicate upper limit of acceptability (Center for Food Safety, 2014).

Table 4: Yeasts and molds count in mango juice during storage

Yeasts and molds count (C FU/ml				
Storage time (month)	**13 °C with preservatives**	**13 °C without preservatives**	**25 °C with preservatives**	**25 °C without preservatives**
0	3.625*103	2.3*104	1.467*104	2.497*103
1	4.3*103	7.05*104	2.825*104	4.2*104
2	1.23*104	2.99*105	2.94*105	1.64*106
3	3.05*105	4.11*105	9.943*105	2.78*107
4	3.25*106	3.66*107	7.49*106	2.72*107

Spoilage in fruits and fruit juices is mostly caused by yeasts contamination mainly due to low acidity. Foods that have low acidity can be spoiled by yeasts because yeasts are most tolerant to acidic conditions being able to grow at pH as low as 2.5 (Praphailong & Fleet, 1997) [12]. It is suggested that spoilage occurs when yeast and mold count reaches 105 cfu/ml. At this limit, color, viscosity, smell and taste of the food are affected by the microorganisms in which case spoilage would have occurred (David & Norah, 1998) [2].

The initial mean population of yeast and molds was 1.4 x 102 cfu/ml (Table 4). At week 6, the mean population was highest, 1.96×108 cfu/ml, in juices stored at (22-25) ºC without preservative and lowest, 1.71 ×104 cfu/ml, in juices stored at (13-16) ºC with preservative. By week 4, all juices, except the chilled with preservative, had yeast counts >105 cfu/ml indicating some degree of spoilage.

Fig 3: Mold and yeast variation, and Colony forming unit of bacterial and fungal cells

Conclusion

These results confirm that temperature and preservatives have significant effects on quality of juice during storage. At higher temperature and without preservative, the juices promoted a faster microbial growth, deteriorated faster in sensory attributes and had a higher rate of quantitative and qualitative loss. A combination of cold storage and use of preservative resulted in highest vitamin C retention during storage. Therefore, based on deterioration of taste, the shelf life were estimated to be two (2) month and four (4) month for juices stored at FARC (22-25) ºC and Haramaya (13-16) ºC respectively. The study underscored the importance of using sensory analysis, particularly attributes like taste and smell, alongside instrumental and microbial analyses in shelf life studies.

Recommendation

Therefore, based on laboratory result and sensory test the upper limit of the prepared mangoes juice was to be 2.5 month and 4 month for at 25 ºC and 13 ºC, respectively. So that any small scale processor can use the processing mango fruit under recommended temperature with listed preservative to extend the shelf life of the juice.

References

1. Centre for Food Safety. Microbiological Guidelines for Food (For ready-to-eat food in general and specific food items). Revised. Food and Environmental Hygiene Department; c2014. http://www.cfs.gov.hk/english/food_leg/files/food_leg_ Microbiological_Guidelines_for_Foo d_e.pdf last accessed: July 2016.

2. Chitedze. Recipes for fruit juice production. Chitedze, Lilongwe, Malawi. David, P. C., & Norah, H. Fruits in Africa. Aspen publishers, UK; c1998.

3. Falade KO, Babalola SO, Akinyemi SOS, Ogunlade AA. Degradation of qualityattributes of sweetened Julie and Ogbomoso mango juices during storage. European Food Research Technology. 2004;218:456-459. http://dx.doi.org/10.1007/s00217-004-0878-5.

4. Guiamba I. Nutritional value and quality of processed mango fruits (Doctoral thesis, Chalmers); c2016.

5. Henney JE, Taylor CL, Boon CS. (Eds). Strategies to reduce sodium intake in the United States. Washington (DC): National Academies Press, USA; c2010. http://dx.doi.org/10.17226/12818.

6. Jahurul MHA, Zaidul ISM, Ghafoor K, Al-Juhaimi FY, Nyam KL, Norulaini NAN, et al. Mango (Mangifera indica L.) by-products and their valuable components: A review. Food chemistry. 2015;183:173-180.

7. Jimenez K, Duran C. Principles of food chemistry (2nd Ed.). University of Guelph, Canada; c1999.

8. Kandasamy P, Shanmugapriya C. Medicinal and nutritional characteristics of fruits in human health. Journal of Medicinal Plants Studies. 2015;4(4):124131.

9. Lawless HT, Heymann H. in Sensory evaluation of food: principles and practices. Chap. 10. Chapman & Hall, New York, NY; c1998. p. 341-378.

10. Lee SK, Kader AA. Preharvest and postharvest factors influencing vitamin C content of horticultural crops. Postharvest biology and technology. 2000;20(3):207220.

11. Liu X. International perspectives on food safety and regulations–a need for harmonized regulations: Perspectives in China. Journal of the Science of Food and Agriculture. 2014;94(10):1928-1931.

12. Lund BM, Collins P, Dimon Z. The microbial safety and quality of foods. Aspen Publishers Ltd, Maryland; c2000.

13. Mahayothee B, Neidhart S, Carle R, Mühlbauer W. Effects of variety, ripening condition and ripening stage on the quality of sulphite-free dried mango slices. European Food Research and Technology.2007;225:723-732.

14. Man D. Food Industry Briefing Aeries: Shelf life. Blackwell Science Ltd, London, UK; c2013. http://dx.doi.org/10.1002/9780470995068.

15. Masamba KG, Mndalira K. Mgaya-Kilima B, Remberg SF, Chove BE, Wicklund T. Food Science & Nutrition. 2014;2(2):181-191. http://dx.doi.org/10.1002/fsn3.97.

16. Masamba KG, Mndalira K. Vitamin C stability in pineapple, guava and baobab juices under different storage conditions using different levels of sodium benzoate and metabisulphite. African Journal of Biotechnology. 2013;12(2).

17. Masibo M, He Q. Major mango polyphenols and their potential significance to human health. Comprehensive reviews in food science and food safety. 2008;7(4):309319.

18. Mkandawire W, Manani TAN, Kabambe OM, Phiri JK.

18. Mkandawire W, Manani TAN, Kabambe OM, Phiri JK. Estimation of Shelf Life of Mango Juice Produced Using Small-Scale Processing Technique. Journal of Food Research. 2016;5(6):13-20.

19. New Zealand Government. https//www.mp.govt.nz/document-vault/3414. Last accessed 2 March 2016; c2014.

20. Panda H. Fruits, Vegetables, Corn and Oilseeds Processing Handbook; c2010.

21. Praphailong W, Fleet GH. Food Microbiology. 1997;14:459-468. http://dx.doi.org/10.1006/fmic.1997.0106.

22. AOAC. Association of Analytical Chemists. Standard Official Methods of Analysis of the Association of Analytical Chemists. 14th edition, S.W Williams (Ed), Washington, DC; c1984. p. 121.

ISSN 2707-8043

Development and evaluation of solar-powered sprayer for large fruit trees pesticide

Jemal Nur
Oromia Agricultural Research Institute, Fedis Agricultural Research Centre, PO Box 904, Harar, Ethiopia
Heykel Jemal
Oromia Agricultural Research Institute, Fedis Agricultural Research Centre, PO Box 904, Harar, Ethiopia
Bayissa Tarecha
Harar Polyphonic College, Automotive Department, PO Box, 67, Harar, Ethiopia

ABSTRACT

The spraying of pesticides is an important task to protect crops from insects for obtaining high yields. The hand-operated sprayer is one of, labour intensive and time-consuming method, which decreases productivity due to low capacity per unit of time. Hence, to overcome this work drudgery design solarpowered faring foliar or pesticide sprayers that solve the best alternate solution and better operation for large fruit trees. Therefore, the aim of this study was to develop and evaluate solar-powered agricultural sprayers for vegetable and fruit trees. The system was designed by considering different parameters; spraying capacity, basic raw material, environmental and crop condition, operating and coverage of area per unit time. The experiment was arranged in factorial Randomized Complete Block Design (RCBD) with six treatments replicated 3 times. Treatments: 3 hose diameter and 3 length hose. The machine has capacity of 0.25 ha/hr. The actual area coverage and discharging rate of 1.32 lit/min, as well as the efficiency of the machine, was 79.4%. This value was coincided with the average fruit tree of the study area. Based on the tested result, the sprayers produce the best booming uniformity and droplet size at six diameters at nine meter (9 m) vertical height that is better technology for large fruit trees like mango and avocado as well as agro-forestry foliar and chemical application and should promote for farming communities boosting agricultural production and productivity.

Keywords: Solar panel, DC battery, DC pump, hose, nozzle, foliar, sprayer

Introduction

Agriculture is a profession of many tedious processes and practices, one of which is the spraying of pesticides in the farm fields. Sprayers are mechanical devices that specifically designed to spray liquids quickly and easily. The spraying of pesticides is an important task in agriculture for protecting the crops from insects and currently used for foliar application.In developing countries like Ethiopia farmers mainly used manual, hand-operated sprayers for this task. This operation conducted through a backpack spraying mechanism, which is fitted with as harnessed human back to carry and operate by

hand. A hand lever continuously operated to maintain pressure makes the backpack sprayers output uniform and handheld sprayers. Basically, this type sprayers are low-cost backpack sprayer which, will generate only low pressure and lack features such as high-pressure pumps, pressure adjustment control (regulator) and pressure gauge found on commercial grade units according to (Joshua et al., 2010) [3]. In fact, high-pressure sprayers, the designed of high-pressure sprayers that fitted with boom they can do any work done by the suitable low-pressure boom sprayers. These can also be fitted with handguns. The handgun is used for spraying shade trees and ornamental, livestock, orchards, building, unwanted brush, rights-of-way, and commercial crops used for reduce drudgery, and hazardous of chemicals (Riley and Siemen, 2003) [1]. Besides high tech. and heavy-duty multipurpose sprayer. Low-cost and multipurpose smallholder farmers were crucially important for large fruit trees and other crop protection. The sprayer of this type was a great way to use for large fruit trees like; mango and Avocado for over height and as well as over ground spraying processes. Hence, rethinking and reversed engineering in developing countries for availing technology options is very important. Conspicuous Solar energy-based pesticides sprayer are the ultimate cost-effective solution at the locations where spraying is difficult.

Materials and Methods

Description of the machine components

The main components of the machine consist of frames, a fluid storage tank and seat, a high-speed DC motor with filter, a battery, a solar panel, a power supply circuit, a hose and a nozzle (Table 1). After the necessary design and specification was completed basic material, selection for construction of the machine/sprayer made. The sprayer manufactured in Fadis Agricultural Research Center, Agricultural Engineering Workshop. Accordingly, the evaluation of manufactured sparer commenced on the papaya, avocado and mango tree in Babile and Fadis districts since 2019. Both districts were situated in East Hararghe zone of Oromia Regional State of 1885 m A.S.L. with a point location of 09018'09" N latitudes and 420 07' 03" longitude respectively

Table 1: Material specification of solar-powered sprayer

Sr. No.	Description	Specification
1	Fluid storage/Tank	PVC, 15-20 Lit
2	Solar panel	20 Watt PV solar panel:- Dimension: 540 x 350 x 25 mm, Weight :1kg, Max voltage:17 V, Max current: 1.18 Amp, Tolerance: ± 5%
3	Charge controller	Capacity 12V, 5Amp
4	Battery	Sealed lead acid battery:- Capacity: 12V, 9 Amph. dimension: 15 x 9 x 6 cm, weight:2.5 kg; max initial current= 2.4 A, cycle use :14.5-14.9 V
5	Motor	Brushless DC motor Capacity:12 V, 1.2 A, :0 - 6000 rpm
6	Hoses	Diameter: 6, 8 and 10 mm diameter types ¼ standard
7	Metal parts	Wheelchair wheel, angle iron, square pipe, electric wire 1.5, metal pipes
8	Switch	Push button type switch
9	Hardener	Epoxy

Solar panel: The solar panel/photovoltaic system can be used to collect solar energy for generating and supplying electricity current. Based on the designed sprayer's power source required selection of solar panels was conducted as described in Table.1

DC motor: High-speed DC motor is used to pressurize and lift fluid from the tank to the required head.

Battery: Is an electrochemical cell storage with externally connected provided to power electrical devices. When a battery is supplying electric power, its positive terminal is the cathode and its negative terminal is the anode.

Storage tank: Storage tank or container used to hold liquid when required spraying on selected crops, or fruit trees. Storage tanks are available, based on type and size; in this case, the selected fluid storage tank was a Knapsack with capacity of 15 liter.

Nozzle: A nozzle is a device designed to control the direction or characteristics of a fluid flow (Krishna, et al. 2017) [6]. A nozzle is often a pipe or tube of varying pressure and fluid viscosity. For this purpose nozzle, selection was done directly from FAO, (2001) [7] standard manuals guide as 110o flat fan type.

Solar panel and tank support frame: It is used to support all the sprayers system and manufactured from angle iron, square pipe and; wheel for movability. The main functions of a frame are to support the tank components and all accessories of sprayers, without undue deflection or distortion.

Nozzle and hose support frame: Manufactured from 30, 25 and 20 mm by 3 mm thick square pipes of 4, 3, and 2.5 m length respectively in accordance of telescopic mode for elongating purposes. At 2 m, vertical height from handlebar jointer fixed together with hollow shaft of 1.27 cm diameter and 25 cm length to insert into 2.54 cm hollow shaft at the top of the vertical arm. The operator at handlebar carried the hose internally and rotate at 3600 guiding the horizontal arm.

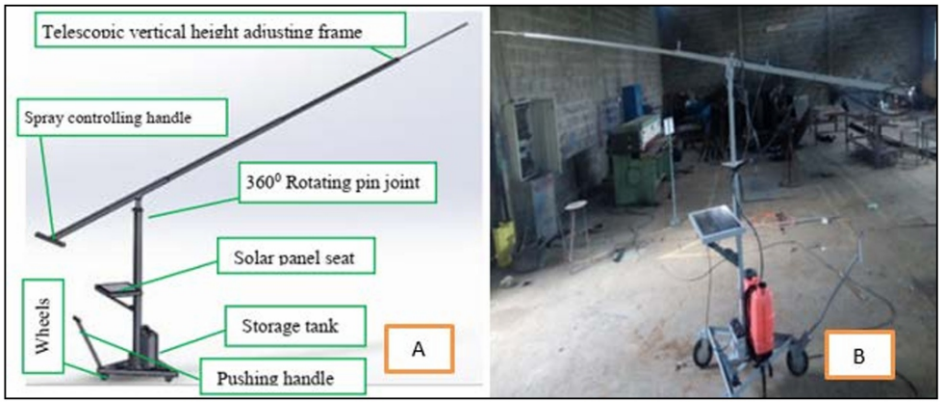

Fig 1: A-3D frame design; B - fully Assembled prototype of solar-powered sprayers

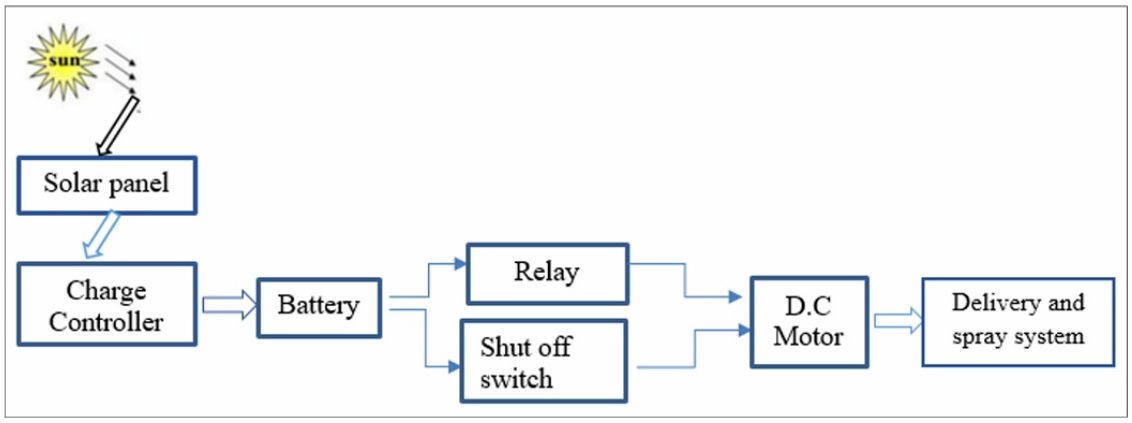

Fig 3: Operation mechanism of solar-powered sprayer

Experimental design and statistical analysis

The experimental has factorial arranged in randomized complete block design (RCBD). The treatments are namely: Three hose diameters (Φ) 6, 8 and 10 mm, and 3-nozzle length/ height positions (3, 6 and 9 meter). Each treatment was replicated three times. All measured variables were subjected to Genstat 15th edition software for analysis of variance. The mean separation made using (LSD) the least significant difference at a 5% level of probability.

Table 2: Experimental treatments

Treatment	Hose Diameter in (mm)	Nozzle Height/Position (m)	Treatment combination
T_1	6	3	6 mm Φ hose at 3 m nozzle height
T_2		6	6 mm Φ hose at 6 m nozzle height
T_3		9	6 mm Φ hose at 9 m nozzle height
T_4	8	3	8 mm Φ hose at 3 m nozzle height
T_5		6	8 mm Φ hose at 6 m nozzle height
T_6		9	8 mm Φ hose at 9 m nozzle height
T_7	10	3	10 mm Φ hose at 3 m nozzle height
T_8		6	10 mm Φ hose at 6 m nozzle height
T_9		9	10 mm Φ hose at 9 m nozzle height

Data collected

Parameters collected during the test include droplet size, boom uniformity, spray height, and discharging rate. In addition to this data total battery charging and discharging time, operating time, spraying capacity and pumping efficiency were collected.

Machine performance

Field capacity: To determine actual field capacity, time consumed for real work and time lost for different activities such as cut-off time, and tank-filling time was taken into consideration. Time required for actual field operation and time lost measured by stopwatch. However, the time lost for recharging the battery, and fixing the sprayer trouble shoot neglected, because usually, it accomplished

before starting fieldwork. Accordingly, for field performance evaluation, the average operation speed is taken from operator. The assumptions coverage area (trees canopy) is in the form of sector of a spherical shape and the operator controls the working path.

$$\text{Actual Field Capacty} = \frac{\text{Actual Area coverd (ha)}}{\text{Total time required to cover ha (hr.)}} \quad (1)$$

$$\text{Theoretical field capacity} = \frac{\text{Theoretical width (m)} * \text{Speed (km/h)}}{10} \quad (2)$$

Power conversion efficiency

Sunlight is converted by solar panels to energy, hence panels' of the solar cell power conversion efficiency was determined according to (Joshua, et al. 2010) [3]. The power calculation is determined according to (Sootha and Gupta, 1991) [4].

Power = Voltage * current

Battery duty/operating time (Bt) calculated by

$$Bt = \frac{\text{Power stored in battery}}{\text{Power Consumed by motor (pump)}} \quad (3)$$

Pump efficiency: It measures how effectively the motor utilizes the power supplied by the battery in delivering with constant pressure to the hose.

$$\text{Pumping efficiency (\%)} = \frac{\text{power required to deliver liquid}}{\text{power supplied by the solar panel}} * 100 \quad (4)$$

Result and Discussion

Determination of solar panel and battery output characteristic

To calculate the output characteristics of the whole system i.e. maximum voltage and current generated denoted by manufacturers' was taken as Vmax.. = 17 and Imax = 1.18 A respectively. Thus the maximum power (Pmax) generated by solar panels as (Pmax= Vmax * I max), which was 20.07 Wh. Similarly, the maximum out power of the battery was calculated in the same manner as 108 Whir. accordingly, battery charging time and fully charged operating time was determined as follows.

Battery maximum charging time is Tmax = Pmax stored by battery divided by Pmax generated by solar panel as 5.4 hr. However, charging time varies with intensity of sun radiations at different rates with respect to the solar panel. Battery operating time depends on load required by the pump unit. Thus, According to manufacturers, the maximum load required by a high-speed DC motor pump as 18 watts. Hence, the maximum battery operating time calculated as the ratio of power stored in the battery to the power consumed by the pump, which was equal to 6 hr.

Pump Efficiency: The power required to deliver liquid was 18 W and the power supplied by solar panel 20.07 W. Thus, the calculated pumping efficiency found as 89.7%. Therefore, the required energy for the designed sprayer is 20 W solar panels and a 12 V DC motor is selected. For continuous power, supply, to the spraying system, equipped with rechargeable battery cell of (12V, 9 Ah) preferably.

Sprayer field efficiency: The sprayer was evaluated on local mango variety having different heights, to actual field capacity, and theoretical field capacity using (equation). The area of the local mango canopy was spherical in shape of average radius of 5 m.

A = 4Πr2 = 314 m2 = 0.0314 ha and time to cover this area = 0.125 hr.

$$= \frac{0.0314 \text{ ha}}{0.125 \text{ hr}} = 0.25 \text{ ha/hr.}$$

$$\text{Theoretical field capacity} = \frac{\text{Theoretical width (m) x Speed (km/h)}}{10}$$

$$= \frac{1.9 \text{ m x } 1.66 \text{ (km/h)}}{10} = 0.315 \text{ ha/hr}$$

$$\text{Field efficiency} = \frac{\text{Actual field capacity}}{\text{Theoretical field capacity}} * 100$$

$$= \frac{0.25}{0.315} * 100 = 79.4\%$$

Field performance of solar power sprayer

Effect of hose length and diameter on droplet size

ANOVA indicated that droplet size of the sprayed fluid was significantly different ($p<0.05$) affected by both hose diameter and length. The larger and lowest droplet size of 2.28 and 0.693 mm, were recorded

by 10 mm hose diameter at 9 m spraying height. This shows that both hose diameter and height of the nozzle have a significant effect on droplet size. Specifically, the result indicated that, as hose diameter increases droplet size increased.

Table 3: Mean values of performance test

Treatment combination	Droplet size (mm)	Boom/Uniformity (inch)	Area Coverage (ha)	Discharge rate lit/min
6 mm Φ hose at 3m length	0.816a	0.53a	1.19c	2.013ab
6 mm Φ hose at 6 m length	0.693a	0.997ab	0.8133bc	1.78ab
6 mm Φ hose at 9 m length	0.927a	1.43ab	0.3567ab	1.32a
8 mm Φ hose at 3m length	1.55[a]	2.263abc	0.1667a	2.8c
8 mm Φ hose at 6 m length	0.827a	1.913ab	0.37ab	1.877ab
8 mm Φ hose at 9 m length	0.787a	2.54bc	0.36ab	2.073b
10 mm Φ hose at 3m length	1.53ab	2.093abc	0.2633ab	2.83c
10 mm Φ hose at 6 m length	1.6ab	2.26abc	0.3867ab	2.037b
10 mm Φ hose at 9m length	2.283b	3.737c	0.1233a	1.527ab
CV (%)	30.7	46.5	68.2	18.3
L.S.D (%)	0.818	1.59	0.5289	0.6423

Effect of hose length and Diameter on boom uniformity

ANOVA indicated that boom uniformity of sprayer fluid was significantly ($p<0.05$) affected by both hose length and diameter. The lowest gap in between droplets (booming uniformity) observed as 0.53 mm from 6 mm diameter of hose at 3 m nozzle vertical length or height, whereas the largest droplet distance was produced as 3.74 mm by 10 mm hose at 9 m length. This shows that the best boom uniformity pattern is produced at the smallest hose diameter and short length, which agrees with the result of (Foques and Nuyttens, 2011a), 255 and 588-micrometre knapsack sprayer booming patterns recorded at laboratory. Generally, booming pattern shows increasing trends as the hose length and diameter increases. Moreover, the accuracy of taking boomed droplet distance measurement affected by natural factors like wind and sun, which resulted in droplet size dropping or expanding more than nature of the boom before measuring.

Effect of hose length and Diameter on area coverage

Area coverage or boom diameter of the sprayer was highly significantly ($p<0.01$) affected by both hose diameter and length. The highest and lowest mean values of area coverage recorded as 1.19 and 0.123 ha by 6 mm and 10 mm hose Φ at 3 m vertical nozzle height respectively (Table 3). This shows that both pipe/hose diameter and length /height have significant effects on fluid pumping capacity of the motor. Moreover, the result revealed that, as hose diameter and length increase flow velocity/pressure decrease or booming capacity of the nozzle decrease, because of pressure loss due to pipe diameter as well as, hose length. This means area coverage has direct relationship with the amount of fluid discharged per unit time of application. Therefore, the selection of optimum area coverage on the bases of hose diameter and length and required discharge economically important, by keeping other parameter (power source and motor capacity) constant. Hence, the optimum area or booming capacity observed,

as 6 m vertical height with 6 mm hose diameter first option followed by 8 and 10 mm as the best to effective spraying capacity per unit time.

Effect of hose length and diameter on discharge

ANOVA revealed that flow rate or discharge of fluid is highly significantly ($p<0.01$) affected by both hose diameter and length. The highest and lowest mean flow rate produced as 2.85 and 1.32 lit/min recorded by 10 mm hose Φ at 3 m length and 6 mm hose Φ at 9 m length respectively. This shows that the flow rate or discharge of fluid was significantly affected nozzle height. Accordingly, as the spraying height position increase discharge rate show decrease trended. This may be due to pressure head loss or friction loss.

Conclusion and Recommendation

As observed from the above result the solar-powered sprayer was best alternative in order to alleviate the problem of spraying on long fruit trees. The sprayer has important spraying merit in relation for selecting right type of spaying head, on the base of hose diameter /nozzle position height. Therefore, the selection of optimum area coverage on the bases of hose diameter and length and required discharge economically important, by keeping other parameter (power source and motor capacity) constant. Hence, the optimum area or booming capacity observed, as 6 m vertical height with 6 mm hose diameter first option followed by 8 and 10 mm as the best to effective spraying capacity per unit time.

Reference

1. Becky Riley, Laurenm Siemen Newman. On the frontline: Health hazard posed to pesticide applicators, restoring healthy school landscapes; c2003. p. 18-24.

2. Foqué D, Nuyttens D. Nozzle Type and Spray Angle Effects on Spray Deposition in Ivy Pot Plants. Pest Management Science. 2011a;67:199-208.

3. R Joshua, V Vasu, P Vincent. Solar Sprayer - An Agriculture Implement International Journal of Sustainable Agriculture. 2010;2(1):16-19.

4. Sootha GD, SK Gupta. Jugal Kishor (Ed.) Solar Energy Centre. Proceedings of the Workshop on Technology Transfer; c1991

5. Nitish Das, Namit Maske. Vinayak Khawas SK, Chaudhary, RD Dhete. Agricultural Fertilizers and Pesticides Sprayers - A Review: IJIRST – International Journal for Innovative Research in Science & Technology. 2015 Apr;1:11 | ISSN (Online): 2349-6010 by www.ijirst.org.

6. Krishna A, Cian L, Aydınoğlu NZ. Sensory aspects of package design. Journal of Retailing. 2017 Mar 1;93(1):43-54.

7. Nebié Y, Meda N, Leroy V, Mandelbrot L, Yaro S, Sombié I, et al. Sexual and reproductive life of women informed of their HIV seropositivity: A prospective cohort study in Burkina Faso. JAIDS Journal of Acquired Immune Deficiency Syndromes. 2001 Dec 1;28(4):367-72.

Instructions for Authors

Essentials for Publishing in this Journal

1 Submitted articles should not have been previously published or be currently under consideration for publication elsewhere.

2 Conference papers may only be submitted if the paper has been completely re-written (taken to mean more than 50%) and the author has cleared any necessary permission with the copyright owner if it has been previously copyrighted.

3 All our articles are refereed through a double-blind process.

4 All authors must declare they have read and agreed to the content of the submitted article and must sign a declaration correspond to the originality of the article.

Submission Process

All articles for this journal must be submitted using our online submissions system. http://enrichedpub.com/ . Please use the Submit Your Article link in the Author Service area.

Manuscript Guidelines

The instructions to authors about the article preparation for publication in the Manuscripts are submitted online, through the e-Ur (Electronic editing) system, developed by **Enriched Publications Pvt. Ltd**. The article should contain the abstract with keywords, introduction, body, conclusion, references and the summary in English language (without heading and subheading enumeration). The article length should not exceed 16 pages of A4 paper format.

Title

The title should be informative. It is in both Journal's and author's best interest to use terms suitable. For indexing and word search. If there are no such terms in the title, the author is strongly advised to add a subtitle. The title should be given in English as well. The titles precede the abstract and the summary in an appropriate language.

Letterhead Title

The letterhead title is given at a top of each page for easier identification of article copies in an Electronic form in particular. It contains the author's surname and first name initial .article title, journal title and collation (year, volume, and issue, first and last page). The journal and article titles can be given in a shortened form.

Author's Name

Full name(s) of author(s) should be used. It is advisable to give the middle initial. Names are given in their original form.

Contact Details

The postal address or the e-mail address of the author (usually of the first one if there are more Authors) is given in the footnote at the bottom of the first page.

Type of Articles

Classification of articles is a duty of the editorial staff and is of special importance. Referees and the members of the editorial staff, or section editors, can propose a category, but the editor-in-chief has the sole responsibility for their classification. Journal articles are classified as follows:

Scientific articles:

1. Original scientific paper (giving the previously unpublished results of the author's own research based on management methods).
2. Survey paper (giving an original, detailed and critical view of a research problem or an area to which the author has made a contribution visible through his self-citation);
3. Short or preliminary communication (original management paper of full format but of a smaller extent or of a preliminary character);
4. Scientific critique or forum (discussion on a particular scientific topic, based exclusively on management argumentation) and commentaries. Exceptionally, in particular areas, a scientific paper in the Journal can be in a form of a monograph or a critical edition of scientific data (historical, archival, lexicographic, bibliographic, data survey, etc.) which were unknown or hardly accessible for scientific research.

Professional articles:

1. Professional paper (contribution offering experience useful for improvement of professional practice but not necessarily based on scientific methods);
2. Informative contribution (editorial, commentary, etc.);
3. Review (of a book, software, case study, scientific event, etc.)

Language

The article should be in English. The grammar and style of the article should be of good quality. The systematized text should be without abbreviations (except standard ones). All measurements must be in SI units. The sequence of formulae is denoted in Arabic numerals in parentheses on the right-hand side.

Abstract and Summary

An abstract is a concise informative presentation of the article content for fast and accurate Evaluation of its relevance. It is both in the Editorial Office's and the author's best interest for an abstract to contain terms often used for indexing and article search. The abstract describes the purpose of the study and the methods, outlines the findings and state the conclusions. A 100- to 250-Word abstract should be placed between the title and the keywords with the body text to follow. Besides an abstract are advised to have a summary in English, at the end of the article, after the Reference list. The summary should be structured and long up to 1/10 of the article length (it is more extensive than the abstract).

Keywords

Keywords are terms or phrases showing adequately the article content for indexing and search purposes. They should be allocated heaving in mind widely accepted international sources (index, dictionary or thesaurus), such as the Web of Science keyword list for science in general. The higher their usage frequency is the better. Up to 10 keywords immediately follow the abstract and the summary, in respective languages.

Acknowledgements

The name and the number of the project or programmed within which the article was realized is given in a separate note at the bottom of the first page together with the name of the institution which financially supported the project or programmed.

Tables and Illustrations

All the captions should be in the original language as well as in English, together with the texts in illustrations if possible. Tables are typed in the same style as the text and are denoted by numerals at the top. Photographs and drawings, placed appropriately in the text, should be clear, precise and suitable for reproduction. Drawings should be created in Word or Corel.

Citation in the Text

Citation in the text must be uniform. When citing references in the text, use the reference number set in square brackets from the Reference list at the end of the article.

Footnotes

Footnotes are given at the bottom of the page with the text they refer to. They can contain less relevant details, additional explanations or used sources (e.g. scientific material, manuals). They cannot replace the cited literature.
The article should be accompanied with a cover letter with the information about the author(s): surname, middle initial, first name, and citizen personal number, rank, title, e-mail address, and affiliation address, home address including municipality, phone number in the office and at home (or a mobile phone number). The cover letter should state the type of the article and tell which illustrations are original and which are not.

Note